REPORT DOCUMENTATION PAGE	Form Approved OMB NO. 0704-0188

The public reporting burden for this collection of information is estimated to average 1 hour per response, including the time for reviewing instructions, searching existing data sources, gathering and maintaining the data needed, and completing and reviewing the collection of information. Send comments regarding this burden estimate or any other aspect of this collection of information, including suggesstions for reducing this burden, to Washington Headquarters Services, Directorate for Information Operations and Reports, 1215 Jefferson Davis Highway, Suite 1204, Arlington VA, 22202-4302. Respondents should be aware that notwithstanding any other provision of law, no person shall be subject to any oenalty for failing to comply with a collection of information if it does not display a currently valid OMB control number.
PLEASE DO NOT RETURN YOUR FORM TO THE ABOVE ADDRESS.

1. REPORT DATE (DD-MM-YYYY)	2. REPORT TYPE	3. DATES COVERED (From - To)
25-05-2014	Final Report	15-Sep-2010 - 14-Sep-2013

4. TITLE AND SUBTITLE	5a. CONTRACT NUMBER
FINAL TECHNICAL REPORT - ADVANCED POLYMER SYSTEMS FOR DEFENCE APPLICATIONS: POWER GENERATION, PROTECTION AND SENSING - ARO W911NF-10-1-0476	W911NF-10-1-0476

5b. GRANT NUMBER

5c. PROGRAM ELEMENT NUMBER
 611104

6. AUTHORS	5d. PROJECT NUMBER
Nicholas Leventis, Massimo Bertino, Frank Blum, Lokesh Dharani, Zhonghua Peng, Chariklia Sotiriou-Leventis, Jeffrey Winiarz, Yangchuan Xing	

5e. TASK NUMBER

5f. WORK UNIT NUMBER

7. PERFORMING ORGANIZATION NAMES AND ADDRESSES	8. PERFORMING ORGANIZATION REPORT NUMBER
Missouri University of Science and Technol 300 W. 12th Street Rolla, MO 65409 -1330	

9. SPONSORING/MONITORING AGENCY NAME(S) AND ADDRESS (ES)	10. SPONSOR/MONITOR'S ACRONYM(S) ARO
U.S. Army Research Office P.O. Box 12211 Research Triangle Park, NC 27709-2211	11. SPONSOR/MONITOR'S REPORT NUMBER(S) 58312-CH.49

12. DISTRIBUTION AVAILIBILITY STATEMENT

Approved for Public Release; Distribution Unlimited

13. SUPPLEMENTARY NOTES
The views, opinions and/or findings contained in this report are those of the author(s) and should not contrued as an official Department of the Army position, policy or decision, unless so designated by other documentation.

14. ABSTRACT

Synthesis of Robust Nanoporous All-Polymer Aerogels as Multifunctional Materials: Demonstrated extremely strong aerogels with polyureas, polyimides, polyamides (KevlarTM-like), polybenzoxazines, poly(acrylonitrile-co-diacrylate), as well as polynorbornene and polydicyclopentadiene. Found that: (a) Fibrous nanostructures are more resilient, rendering fibrous polymeric aerogels the most desirable for applications; and, (b) Both particulate and fibrous nanostructures consist of about the same-size primary and secondary particles. Hence, controlling formation of nano-fibers becomes a task of directing the assembly of secondary nanoparticles into strings. Collateral benefits

15. SUBJECT TERMS

Aerogels, X-aerogels, nanostructured, crosslinked, ceramics, graphite, polymers, vanadia, polyurea, polyurethanes, polyamides, polyimides, polybenzoxazine, polyacrylonitrile, polyaniline, ROMP, flame synthesis, sensors, amines

16. SECURITY CLASSIFICATION OF:			17. LIMITATION OF ABSTRACT	15. NUMBER OF PAGES	19a. NAME OF RESPONSIBLE PERSON Nicholas Leventis
a. REPORT	b. ABSTRACT	c. THIS PAGE	UU		19b. TELEPHONE NUMBER 573-341-4391
UU	UU	UU			

Standard Form 298 (Rev 8/98)
Prescribed by ANSI Std. Z39.18

Report Title

FINAL TECHNICAL REPORT - ADVANCED POLYMER SYSTEMS FOR DEFENCE APPLICATIONS: POWER GENERATION, PROTECTION AND SENSING - ARO W911NF-10-1-0476

ABSTRACT

Synthesis of Robust Nanoporous All-Polymer Aerogels as Multifunctional Materials: Demonstrated extremely strong aerogels with polyureas, polyimides, polyamides (KevlarTM-like), polybenzoxazines, poly(acrylonitrile-co-diacrylate), as well as polynorbornene and polydicyclopentadiene. Found that: (a) Fibrous nanostructures are more resilient, rendering fibrous polymeric aerogels the most desirable for applications; and, (b) Both particulate and fibrous nanostructures consist of about the same-size primary and secondary particles. Hence, controlling formation of nano-fibers becomes a task of directing the assembly of secondary nanoparticles into strings. Collateral benefits include: (a) Regioselective cross-linking of silica with magnesium silicate ceramics; (b) Efficient synthesis for nanofibrous vanadia from vanadium oxytricholoride [$VOCl_3$] cutting the cost of vanadia aerogels by a factor of 10 (cheaper than silica); (c) Polymer coated oxide nanoparticles synthesized via non-sol-gel methods, e.g., via a flame process; and, (d) Amine sensors based on silver nanoparticle-doped polyaniline.

Development and Self-Assembly of Multifunctional Inorganic-Polymer Hybrid Materials for Solar Energy Applications: Demonstrated convenient synthesis of various semiconducting nanoparticles, studied functionalized polyoxometalates (POMs), and developed novel conjugated systems with foldamers and dendrimers. Demonstrated that surface charged nanoparticles can self-assemble into thermodynamically stable single-shell hollow nanovesicles with applications as photocatalysts for solar water splitting and as traceable drug carriers. Synthesized the first hybrid rod-coil diblock copolymers with POM clusters covalently attached to the coil block, and demonstrated unique solution self-assembly behavior and photovoltaic properties. Synthesized new polycyclic aromatic compounds that can be solution processed into thin films with unusually high hole mobility. Such molecules coated on nanofibers consisting of electron acceptors behave as photoinduced electron donors yielding significantly enhanced photocurrent. Designed new low band-gap donor-acceptor conjugated polymers demonstrating good solar cell performances. Demonstrated that mechanical alloying can be used to prepare carbon nanodots, which can be used as interfacial layer in hybrid solar cells with dramatically improved short circuit currents.

Enter List of papers submitted or published that acknowledge ARO support from the start of the project to the date of this printing. List the papers, including journal references, in the following categories:

(a) Papers published in peer-reviewed journals (N/A for none)

<u>Received</u>	<u>Paper</u>
04/21/2013 23.00	Dhairyashil P. Mohite, Zachary J. Larimore, H. Lu, Joseph T. Mang, Chariklia Sotiriou-Leventis, Nicholas Leventis. Monolithic Hierarchical Fractal Assemblies of Silica Nanoparticles Cross-Linked with Polynorbornene via ROMP: A Structure–Property Correlation from Molecular to Bulk through Nano, Chemistry of Materials, (09 2012): 3434. doi: 10.1021/cm3017648
04/21/2013 30.00	Mingzhen Yao, Ryan Hall, Wei Chen, Dhairyashil P. Mohite, Nicholas Leventis, Ning Lu, Jinguo Wang, Moon J. Kim, Huiyang Luo, Hongbing Lu. Luminescent LaF3:Ce-doped organically modified nanoporous silica xerogels, Journal of Applied Physics, (01 2013): 13111. doi: 10.1063/1.4773330
04/21/2013 29.00	Shruti Mahadik-Khanolkar, Huiyang Luo, Hongbing Lu, Chariklia Sotiriou-Leventis, Nicholas Leventis, Dhairyashil P. Mohite. Polydicyclopentadiene aerogels grafted with PMMA: II. Nanoscopic characterization and origin of macroscopic deformation, Soft Matter, (03 2013): 1531. doi: 10.1039/c2sm27606b
04/21/2013 28.00	Dhairyashil P. Mohite, Shruti Mahadik-Khanolkar, Huiyang Luo, Hongbing Lu, Chariklia Sotiriou-Leventis, Nicholas Leventis. Polydicyclopentadiene aerogels grafted with PMMA: I. Molecular and interparticle crosslinking, Soft Matter, (03 2013): 0. doi: 10.1039/c2sm26931g
04/21/2013 27.00	Anand G. Sadekar, Dhairyashil Mohite, Sudhir Mulik, Naveen Chandrasekaran, Chariklia Sotiriou-Leventis, Nicholas Leventis. Robust PEDOT films by covalent bonding to substrates using in tandem sol–gel, surface initiated free-radical and redox polymerization, Journal of Materials Chemistry, (01 2012): 100. doi: 10.1039/c1jm12563j
04/21/2013 26.00	Charles Wingfield, Louis Franzel, Massimo F. Bertino, Nicholas Leventis. Fabrication of functinally graded aerogels, cellular aerogels and anisotropic ceramics, J Materials Chemistry, (08 2011): 11737. doi:
04/21/2013 25.00	Anand G. Sadekar, Shruti S. Mahadik, Abhishek N. Bang, Zachary J. Larimore, Clarissa A. Wisner, Massimo F. Bertino, A. Kaan Kalkan, Joseph T. Mang, Chariklia Sotiriou Leventis, Nicholas Leventis. From 'Green' Aerogels to Porous Graphite by Emulsion Gelation of Acrylonitrile, Chemistry of Materials, (01 2012): 26. doi: 10.1021/cm202975p
04/21/2013 24.00	Arumugam Thangavel, Chariklia Sotiriou Leventis, Richard Dawes, Nicholas Leventis. Orientation of Pyrylium Guests in Cucurbituril Hosts, The Journal of Organic Chemistry, (03 2012): 2263. doi: 10.1021/jo202434z
04/22/2013 31.00	Zhe-Fei Li, Frank D. Blum, Massimo F. Bertino, Chang-Soo Kim. Amplified response and enhanced selectivity of metal-PANI fiber composite based vapor sensors, Sensors and Actuators B: Chemical, (01 2012): 390. doi: 10.1016/j.snb.2011.10.049
04/22/2013 34.00	Yong Li, Peifen Lu, Minlin Jiang, Rabin Dhakal, Prem Thapaliya, Zhonghua Peng, Binay Jha, Xingzhong Yan. Femtosecond Time-Resolved Fluorescence Study of TiO, The Journal of Physical Chemistry C, (12 2012): 25248. doi: 10.1021/jp3094897
04/22/2013 33.00	Zhe-Fei Li, Frank D. Blum, Massimo F. Bertino, Chang-Soo Kim. Understanding The Response of Nanostructured Polyaniline Gas Sensors, Sensors and Actuators B: Chemical, (04 2013): 0. doi: 10.1016/j.snb.2013.03.125

04/22/2013 32.00 Tan Zhang, Gu Xu, Jim Puckette, Frank D. Blum. Effect of Silica on the Structure of
Cetyltrimethylammonium Bromide,
The Journal of Physical Chemistry C, (05 2012): 11626. doi: 10.1021/jp303338t

04/23/2013 36.00 Guolong Tan, Shaohua Li, James B. Murowchick, Clarissa Wisner, Nickolas Leventis, Zhonghua Peng.
Preparation of uncapped CdSe1?xSx semiconducting nanocrystals by mechanical alloying,
Journal of Applied Physics, (12 2011): 124306. doi: 10.1063/1.3669443

04/23/2013 46.00 Lena Weigold, Dhairyashil P. Mohite, Shruti Mahadik-Khanolkar, Nicholas Leventis, Gudrun Reichenauer.
Correlation of microstructure and thermal conductivity in nanoporous solids: The case of polyurea
aerogels synthesized from an aliphatic tri-isocyanate and water,
Journal of Non-Crystalline Solids, (05 2013): 105. doi: 10.1016/j.jnoncrysol.2013.02.029

04/23/2013 44.00 L. Franzel, C. Wingfield, M. F. Bertino, S. Mahadik-Khanolkar, N. Leventis. Regioselective cross-linking of
silica aerogels with magnesium silicate ceramics,
, (04 2013): 6061. doi: 10.1039/c3ta90165c

04/23/2013 42.00 Mahuya Bagui, Tanmoy Dutta, Haizhen Zhong, Shaohua Li, Sanjiban Chakraborty, Andrew Keightley,
Zhonghua Peng. Synthesis and optical properties of perylene diimide derivatives with triphenylene-based
dendrons linked at the bay positions through a conjugated ethynyl linkage,
Tetrahedron, (04 2012): 2806. doi: 10.1016/j.tet.2012.02.008

04/23/2013 41.00 Yucong Liu, Jiayu He, Osung Kwon, Da-Ming Zhu. Probing local surface conductance using current
sensing atomic force microscopy,
Review of Scientific Instruments, (01 2012): 13701. doi: 10.1063/1.3673476

04/23/2013 43.00 Osung Kwon, Shijie Wu, Da-Ming Zhu. Effect of Thermal Annealing on Proton Conduction in Ion
Exchange Membranes,
MRS Proceedings, (07 2011): 1. doi: 10.1557/opl.2011.1199

04/23/2013 40.00 Tanmoy Dutta, Yanke Che, Haizhen Zhong, John H. Laity, Vladimir Dusevich, James B. Murowchick, Ling
Zang, Zhonghua Peng. Synthesis and self-assembly of triphenylene-containing conjugated macrocycles,
RSC Advances, (04 2013): 6008. doi: 10.1039/c3ra23421e

04/23/2013 38.00 Kuo-Sung Liao, Hongmin Chen, Somia Awad, Jen-Pwu Yuan, Wei-Song Hung, Kuier-Rarn Lee, Juin-Yih
Lai, Chien-Chieh Hu, Y. C. Jean. Determination of Free-Volume Properties in Polymers Without
Orthopositronium Components in Positron Annihilation Lifetime Spectroscopy,
Macromolecules, (09 2011): 0. doi: 10.1021/ma201324k

04/23/2013 39.00 Somia Awad, H. M. Chen, Brian P. Grady, Abhijit Paul, Warren T. Ford, L. James Lee, Y. C. Jean.
Positron Annihilation Spectroscopy of Polystyrene Filled with Carbon Nanomaterials,
Macromolecules, (01 2012): 933. doi: 10.1021/ma202458c

04/23/2013 37.00 Hong Min Chen, J. David Van Horn, Yan Ching Jean. Applications of Positron Annihilation Spectroscopy
to Life Science,
Defect and Diffusion Forum, (09 2012): 275. doi: 10.4028/www.scientific.net/DDF.331.275

04/23/2013 35.00 Sanjiban Chakraborty, Lu Jin, Yong Li, Yucong Liu, Tanmoy Dutta, Da-Ming Zhu, Xingzhong Yan, Andrew
Keightley, Zhonghua Peng. Synthesis, Characterizations, and Morphological Studies of Polyoxometalate-
Containing Rod-Coil Diblock Copolymers,
European Journal of Inorganic Chemistry, (04 2013): 1799. doi: 10.1002/ejic.201201127

08/25/2011 1.00 Nicholas Leventis, Chakkaravarthy Chidambareswarapattar, Dhairyashil P. Mohite, Zachary J. Larimore,
Hongbing Lu, Chariklia Sotiriou-Leventis. Multifunctional porous aramids (aerogels) by efficient reaction of
carboxylic acids and isocyanates,
Journal of Materials Chemistry, (07 2011): 0. doi: 10.1039/c1jm11472g

08/25/2011 3.00 Nicholas Leventis, Chariklia Sotiriou-Leventis, Dhairyashil P. Mohite, Zachary J. Larimore, Joseph T.
Mang, Gitogo Churu, Hongbing Lu. Polyimide Aerogels by Ring-Opening Metathesis Polymerization
(ROMP),
Chemistry of Materials, (04 2011): 2250. doi: 10.1021/cm200323e

08/25/2011 4.00 Charles. Wingfield, Louis. Franzel, Massimo. F. Bertino, Nicholas. Leventis. Fabrication of functionally graded aerogels, cellular aerogels and anisotropic ceramics,
Journal of Materials Chemistry, (07 2011): 11737. doi: 10.1039/c1jm10898k

08/25/2011 5.00 Somia Awad, Hongmin Chen, Guodong Chen, Xiaohong Gu, James L. Lee, E. E. Abdel-Hady, Y. C. Jean. Free Volumes, Glass Transitions, and Cross-Links in Zinc Oxide/Waterborne Polyurethane Nanocomposites,
Macromolecules, (01 2011): 29. doi: 10.1021/ma102366d

08/25/2011 6.00 Dmitry Baranov, Ekaterina N. Kadnikova. Synthesis and characterization of azidoalkyl-functionalized gold nanoparticles as scaffolds for "click"-chemistry derivatization,
Journal of Materials Chemistry, (03 2011): 6152. doi: 10.1039/c1jm10183h

08/25/2011 7.00 Mahuya Bagui, Tanmoy Dutta, Sanjiban Chakraborty, Joseph S. Melinger, Haizhen Zhong, Andrew Keightley, Zhonghua Peng. Synthesis and Optical Properties of Triphenylene-Based Dendritic Donor Perylene Diimide Acceptor Systems,
The Journal of Physical Chemistry A, (03 2011): 1579. doi: 10.1021/jp1085334

08/25/2011 8.00 Osung Kwon, Shijie Wu, Da-Ming Zhu. Configuration Changes of Conducting Channel Network in Nafion Membranes due to Thermal Annealing,
The Journal of Physical Chemistry B, (11 2010): 14989. doi: 10.1021/jp108163a

08/25/2011 9.00 Nicholas Leventis, Chariklia Sotiriou-Leventis, Naveen Chandrasekaran, Sudhir Mulik, Zachary J. Larimore, Hongbing Lu, Gitogo Churu, Joseph T. Mang. Multifunctional Polyurea Aerogels from Isocyanates and Water. A Structure?Property Case Study,
Chemistry of Materials, (12 2010): 6692. doi: 10.1021/cm102891d

08/25/2011 16.00 Massimo F. Bertino, L. Franzel. Inhomogeneous Aerogels,
Review of nanoscience and nanotechnology, (10 2011): 0. doi:

08/25/2011 17.00 Michelle M. Paquette, Wenjing Li, M Sky Driver, Sudarshan Karki, Anthony N Caruso, Nathan A Oyler. The local physical structure of amorphous hydrogenated boron carbide: insights from magic angle spinning solid-state NMR spectroscopy,
J. Phys.: Condens. Matter, (10 2011): 0. doi:

TOTAL: **33**

Number of Papers published in peer-reviewed journals:

(b) Papers published in non-peer-reviewed journals (N/A for none)

<u>Received</u>   <u>Paper</u>

08/25/2011 11.00 Anand Sadakar, Abhishek Bang, Chariklia Sotiriou-Leventis, Nicholas Leventis. Mechanically strong acrylonitrile-based aerogels via free radical polymerization and their conversion to porous carbns, Polymeric Materials Science and Engineering, (04 2011): 576. doi:

08/25/2011 12.00 Shruti S. Mahadik, Naveen Chandrasekaran, Sudhir Mulik, Zachary J. Larimore, Gitogo Churu, Hongbing Lu, Joseph T. mang, Chariklia Sotiriou-Leventis, Nicholas Leventis. Functionally graded polyurea aerogels: synthesis and characterization, Polymer Preprints, (04 2011): 265. doi:

08/25/2011 13.00 Dhairyashil Mohite, Zachary Larimore, Gitogi Churu, Hongbing Lu, Chariklia Sotiriou-Leventis, Nicholas Leventis. Polyimide aerogels by ring opening metathesis polymerization (ROMP), Polymer Preprints, (04 2011): 263. doi:

08/25/2011 14.00 . Polydicyclopentadiene aerogels grafted with polymethylmethacrylate, Polymer Preprints, (09 2011): 0. doi:

08/25/2011 15.00 Abhishek Bang, Anand Sadekar, Brice Curtin, Clayton Buback, Selin Acar, Nicholas Leventis, Chariklia Sotiriou-Leventis. Silica and dysprosia aerogels as drug delivery carriers for indomethacin and paracetamol, Polymer Preprints, (09 2011): 0. doi:

    TOTAL: **5**

Number of Papers published in non peer-reviewed journals:

(c) Presentations

Number of Presentations: 0.00

Non Peer-Reviewed Conference Proceeding publications (other than abstracts):

<u>Received</u>   <u>Paper</u>

    TOTAL:

Number of Non Peer-Reviewed Conference Proceeding publications (other than abstracts):

Peer-Reviewed Conference Proceeding publications (other than abstracts):

Received   Paper

04/23/2013 45.00 Chakkaravarthy Chidambareswarapattar, Zachary Larimore, Chariklia Sotiriou-Leventis, Nicholas Leventis. Mechanically Strong nanoporous Polyimides (Aerogels) from Anhydrides and Isocyanates: A Structure-Proporty Study,
243rd National ACS Meeting (San Diego 2012). 28-MAR-12, . : ,

08/25/2011 18.00 Osung Kwon, Shijie Wu, Da-Ming Zhu. Effect of thermal annealing on proton conduction in ion exchange membranes,
Materials Research Society. , . : ,

08/26/2011 19.00 Nicholas Leventis, Chariklia Sotiriou-Leventis, Naveen Chandrasekaran, Sudhir Mulik, Chakkaravarthy Chidambareswarapattar, Anand Sadekar, Dhairyashil Mohite, Shruti S. Mahadik, Zachary J. Larimore, Hongbing Lu, Gitogo Churu, Joseph T. Mang. Isocyanate derived organic aerogels: polyureas, polyimides, polyamides,
Fall 2010 Materials Research Society Meeting. 29-NOV-10, . : ,

    TOTAL: **3**

Number of Peer-Reviewed Conference Proceeding publications (other than abstracts):

(d) Manuscripts

Received   Paper

08/25/2011 20.00 Anand G. Sadekar, Sudhir Mulik, Naveen Chandrasekaran, Chariklia Sotiriou-Leventis, Nicholas Leventis. Robust PEDOT films by covalent bonding to substrates using in tandem sol-gel, surface initiated free-radical and redox polymerization,
Journal of Materials Chemistry (08 2011)

08/26/2011 21.00 Anand G. Sadekar, Shruti S. Mahadik, Abhishek N. Bang, Zachary J. Larimore, Clarissa A. Wisner, Massimo F. Bertino, Joseph T. Mang, Chariklia Sotiriou-Leventis, Nicholas Leventis. "Green" aerogels and porous carbons by emulsion gelation of acrylonitrile,
Chemistry of Materials (08 2011)

08/26/2011 22.00 Zei-Fei Li, Frank D. Blum, Massimo F. Bertino, Chang-Soo Kim. Amplified response and enhanced selectivity of metal-PANI fiber composite based vapor sensors,
Sensors and Actuators (08 2011)

    TOTAL: **3**

Number of Manuscripts:

Books

08/25/2011 10.00 Nicholas Leventis. Interpenetrating Organic/Inorganic Networks of resorcinol-Formaldehyde/Metal Oxide Aerogels, Chapter14 in Aerogels Handbook, M. Aegerter, N. Leventis, M. Koebel Ed.s, United States: Springer, (06 2011)

08/25/2011 2.00 Nicholas Leventis, Hongbing Lu. Polymer-Crosslinked Aerogels, Chapter 13 in Aerogels Handbook, M. Aegerter, N. Leventis, M. Koebel Ed.s, New York, NY: Springer New York, (06 2011)

    TOTAL: **2**

Patents Submitted

Patents Awarded

Awards

Graduate Students

NAME	PERCENT_SUPPORTED	Discipline
Anand Sadekar	0.50	
Dhairyashil P. Mohite	0.50	
C. Chidambareswarappattar	0.50	
Shruti Mahadik	0.50	
Clarissa Wisner	0.10	
Tyler Fears	0.50	
Vishwanath Gandikota	0.50	
Litao Yan	0.08	
Arumugam Thangavel	0.50	
Tanmoy Dutta	0.50	
Shaohua Li	0.50	
Chingen Chou	0.50	
Mahuya Bagui	0.50	
Sky M. Drive	0.50	
Robert Clevenger	0.50	
Xinyan Bai	0.50	
Kegan Nelson	0.50	
Jessica Robinson	0.50	
Osung Kwon	0.00	
Yuchong Liu	0.00	
Zhe-Fei Li	0.00	
Shadi Alizadeh-Bazazi	0.17	
Mahubha Arachilage	0.13	
Tan Zhang	0.48	
Seyyed Hamid Mortazavian	0.21	
Charmaine V. Munro	0.19	
Bal Khatiwada	0.29	
Madduma Perera	0.02	
Charles Wingfield	0.10	
Louis Franzel	0.10	
Naveen Chandrasekaran	0.50	
Jared Loebs	0.50	
Victoria Prokopf	0.50	
Adnan Malik Saeed	0.50	
Abhishek Bang	0.50	
FTE Equivalent:	**12.37**	
Total Number:	**35**	

Names of Post Doctorates

NAME	PERCENT_SUPPORTED
Yong Li (UMKC)	1.00
Runwu Zhang (UMKC)	1.00
Guolong Tan	1.00
FTE Equivalent:	**3.00**
Total Number:	**3**

Names of Faculty Supported

NAME	PERCENT_SUPPORTED	National Academy Member
Nicholas Leventis	0.10	
Charilia Sotiriou-Leventis	0.05	
Jeffrey Winiarz	0.05	
Lokeswarappa R. Dharani	0.05	
Yangchuan Xing	0.05	
Zhonghua Peng	0.10	
Frank Blum	0.10	
Massimo Bertino	0.05	
FTE Equivalent:	**0.55**	
Total Number:	**8**	

Names of Under Graduate students supported

NAME	PERCENT_SUPPORTED	Discipline
Zachary Larimore	0.20	Mechanical Engineering (MS&T)
Clayton Buback	0.10	Chemical Engineering (MS&T)
Patrick McCarver	0.10	Chemical Engineering (MS&T)
Anthony Tedeschi	0.00	Neuclear Engineering (MS&T)
Brice Curtin	0.00	Chemistry (MS&T)
Selin Acar	0.00	Chemistry (MS&T)
Cody Woodall	0.00	Chemistry (UMKC)
Michael Stumpf	0.00	Chemistry (UMKC)
Brian McEntee	0.00	Chemistry (UMKC)
Mark Rayhart	0.00	Chemistry (UMKC)
Andrew Thome	0.00	Chemistry (UMKC)
Yen Bui	0.00	Chemistry (UMKC)
Ingrid Hsiung	0.00	Chemsitry (UMKC)
Jordan Davis	0.00	Chemistry (UMKC)
Gautam Anand	0.00	Chemistry (UMKC)
Morgan Kohls	0.00	Chemistry (UMKC)
Dean Merrill	0.00	Chemsitry (UMKC)
Zachary Butz	0.00	Chemistry (UMKC)
Richard Wu	0.00	Chemistry (UMKC)
Kennette Pen	0.00	Chemistry (UMKC)
Christopher Brett	0.00	Chemistry (UMKC)
Vladimir I. Kulish	0.00	Chemistry (UMKC)
FTE Equivalent:	**0.40**	
Total Number:	**22**	

Student Metrics

This section only applies to graduating undergraduates supported by this agreement in this reporting period

The number of undergraduates funded by this agreement who graduated during this period: 21.00

The number of undergraduates funded by this agreement who graduated during this period with a degree in science, mathematics, engineering, or technology fields:······ 21.00

The number of undergraduates funded by your agreement who graduated during this period and will continue to pursue a graduate or Ph.D. degree in science, mathematics, engineering, or technology fields:······ 14.00

Number of graduating undergraduates who achieved a 3.5 GPA to 4.0 (4.0 max scale):...... 21.00

Number of graduating undergraduates funded by a DoD funded Center of Excellence grant for Education, Research and Engineering:...... 0.00

The number of undergraduates funded by your agreement who graduated during this period and intend to work for the Department of Defense 1.00

The number of undergraduates funded by your agreement who graduated during this period and will receive scholarships or fellowships for further studies in science, mathematics, engineering or technology fields:...... 14.00

Names of Personnel receiving masters degrees

NAME
Vishwanath Gandikota (Chem. E., MS
Litao Yan (Chem. E., MS&T)
Jared Loebs (ME, MS&T)
Victoria Prokopf (ME, MS&T)
Kegan Nelson (Chemistry, UMKC)
Jessica Robinson (Chemistry, UMKC
Osung Kwon (Chemistry, UMKC)
Yochong Liu (Chemistry, UMKC)
Charles Wingfield (Physics, VCU)
Louis Franzel (Physics, VCU)

Total Number: 10

Names of personnel receiving PHDs

NAME
Anand Sadekar (2011)
Naveen Chandrasekaran (2011)
C. Chidambareswarapattar (MS&T)
Clarissa Wisner (MS&T
Shruti Mahadik-Khanolkar (MS&T)
Dhairyashil Mohite (MS&T)
Arumugam Thangavel (MS&T)
Tanmoy Dutta (UMKC)
Shaohua Li (UMKC)
Chingen Chou (UMKC)
Sky M. Drive (UMKC)
Xinyan Bai (UMKC)
Zhe-Fei Li (OSU)

Total Number: 13

Names of other research staff

NAME	PERCENT_SUPPORTED

FTE Equivalent:
Total Number:

Sub Contractors (DD882)

1 a. Oklahoma State University

1 b. 203 Whitehurst

Stillwater OK 740781016

Sub Contractor Numbers (c):
Patent Clause Number (d-1):
Patent Date (d-2):
Work Description (e):
Sub Contract Award Date (f-1):
Sub Contract Est Completion Date(f-2):

---

1 a. Oklahoma State University

1 b. Research Administration
201 Advanced Technology Research
Stillwater OK 740781016

Sub Contractor Numbers (c):
Patent Clause Number (d-1):
Patent Date (d-2):
Work Description (e):
Sub Contract Award Date (f-1):
Sub Contract Est Completion Date(f-2):

---

1 a. Virginia Commonwealth University

1 b. 800 East Leigh Street, Suite 3200
P.O. Box 980568
Richmond VA 232980568

Sub Contractor Numbers (c):
Patent Clause Number (d-1):
Patent Date (d-2):
Work Description (e):
Sub Contract Award Date (f-1):
Sub Contract Est Completion Date(f-2):

---

1 a. Virginia Commonwealth University

1 b. Box 568, MCV Station
910 W. Franklin St.
Richmond VA 232849004

Sub Contractor Numbers (c):
Patent Clause Number (d-1):
Patent Date (d-2):
Work Description (e):
Sub Contract Award Date (f-1):
Sub Contract Est Completion Date(f-2):

Inventions (DD882)

5 **Efficient synthesis of nanoporous vanadium oxide networks from vanadiium halides**

Patent Filed in US? (5d-1) Y

Patent Filed in Foreign Countries? (5d-2)   N

Was the assignment forwarded to the contracting officer? (5e) N

Foreign Countries of application (5g-2):

    5a: Nicholas Leventis

  5f-1a: MS&T

   5f-c: Dept of Chemistry, MS&T

      Rolla, MO 65401   MO   65409

    5a: Chariklia Sotiriou-Leventis

  5f-1a: MS&T

   5f-c: Dept of Chemistry, MS&T

      Rolla, MO 65401   MO   65409

    5a: Jeffrey Winiarz

  5f-1a: MS&T

   5f-c: Dept of Chemistry, MS&T

      Rolla, MO 65401   MO   65409

    5a: Tyler Fears

  5f-1a: MS&T

   5f-c: Dept of Chemistry, MS&T

      Rolla, MO 65401   MO   65409

5 **Fexible superhydrophobic nanoporous polyurea for thermal insulation and oil-spill remediation**

Patent Filed in US? (5d-1) N

Patent Filed in Foreign Countries? (5d-2)   N

Was the assignment forwarded to the contracting officer? (5e) N

Foreign Countries of application (5g-2):

    5a: Nicholas Leventis

  5f-1a: MS&T

   5f-c: Dept of Chemistry, MS&T

      Rolla, MO 65401   MO   65409

    5a: Chariklia Sotiriou-Leventis

  5f-1a: MS&T

   5f-c: Dept of Chemistry, MS&T

      Rolla, MO 65401   MO   65409

5a: Chakkaravarthy Chidambarwewarappattar

5f-1a: MS&T

5f-c: Dept of Chemistry, MS&T

Rolla, MO 65401   MO   65409

5   **Flexible to rigid nanoporous polyurethane-acrylate (PUAC) type materials for structural and thermal insulation applicatio**

Patent Filed in US? (5d-1)   Y

Patent Filed in Foreign Countries? (5d-2)   N

Was the assignment forwarded to the contracting officer? (5e)   N

Foreign Countries of application (5g-2):

5a: Nicholas Leventis

5f-1a: MS&T

5f-c: Dept of Chemistry, MS&T

Rolla, MO 65401   MO   65409

5a: Abhishek Bang

5f-1a: MS&T

5f-c: Dept of Chemistry, MS&T

Rolla, MO 65401   MO   65409

5a: Chariklia Sotiriou-Leventis

5f-1a: MS&T

5f-c: Dept of Chemistry, MS&T

Rolla, MO 65401   MO   65409

5   **Low-cost lightweight organic aerogel materials for high transmission loss applications**

Patent Filed in US? (5d-1)   Y

Patent Filed in Foreign Countries? (5d-2)   N

Was the assignment forwarded to the contracting officer? (5e)   N

Foreign Countries of application (5g-2):

5a: Nicholas Leventis

5f-1a: MS&T

5f-c: Dept of Chemistry, MS&T

Rolla, MO 65401   MO   65409

5a: Hongbing Lu

5f-1a: University of Texas - Dallas

5f-c: Dept of Mechanical Engineering

Richardson   TX

5a: Ning Xiang

5f-1a: RPI

5f-c: Dept of Electrical Engineering

Troy   NY

5   Multifunctional porous aramids (aerogels) and fabrication thereof

Patent Filed in US? (5d-1) Y

Patent Filed in Foreign Countries? (5d-2) N

Was the assignment forwarded to the contracting officer? (5e) N

Foreign Countries of application (5g-2):

    5a: Chariklia Sotiriou-Leventis

  5f-1a: MS&T

   5f-c: Dept of Chemistry, MS&T

      Rolla, MO 65401   MO   65409

    5a: Chakkaravarthy Chidambarwewarappattar

  5f-1a: MS&T

   5f-c: Dept of Chemistry, MS&T

      Rolla, MO 65401   MO   65409

    5a: Nicholas Leventis

  5f-1a: MS&T

   5f-c: Dept of Chemistry, MS&T

      Rolla, MO 65401   MO   65409

5   Time-efficient, energy efficient acid catalyzed polybenzoxazines

Patent Filed in US? (5d-1) N

Patent Filed in Foreign Countries? (5d-2) N

Was the assignment forwarded to the contracting officer? (5e) N

Foreign Countries of application (5g-2):

    5a: Nicholas Leventis

  5f-1a: MS&T

   5f-c: Dept of Chemistry, MS&T

      Rolla, MO 65401   MO   65409

    5a: Shruti Mahadik-Khanolkar

  5f-1a: MS&T

   5f-c: Dept of Chemistry, MS&T

      Rolla, MO 65401   MO   65409

    5a: Chariklia Sotiriou-Leventis

  5f-1a: MS&T

   5f-c: Dept of Chemistry, MS&T

      Rolla, MO 65401   MO   65409

Scientific Progress

Technology Transfer

FINAL TECHNICAL REPORT

ADVANCED POLYMER SYSTEMS FOR DEFENCE APPLICATIONS:
POWER GENERATION, PROTECTION AND SENSING

ARO W911NF-10-1-0476

May 1, 2014

PERFORMING ORGANIZATIONS

Missouri University of Science and Technology (Lead)
    PI: **Nicholas Leventis – Chemistry**
    Co-PIs:
            Chariklia Sotiriou-Leventis – Chemistry
            Lokeswarappa Dharani – Mechanical Engineering
            Jeffrey Winiarz – Chemistry
            Yangchuan Xing – Chemical Engineering

University of Missouri – Kansas City (Co-Lead)
    PI: **Zhonghua Peng - Chemistry**

Oklahoma State University (Sub-Contractor)
    PI: **Frank Blum - Chemistry**

Virginia Commonwealth University (Sub-Contractor)
    PI: **Massimo Bertino - Physics**

Executive Summary

Missouri University of Science and Technology (Lead Organization)

N. Leventis / C. Sotiriou-Leventis
Synthesis of Robust Nanoporous All-Polymer Aerogels as Multifunctional Materials for Acoustic and Thermal Insulation and Energy Absorption Applications

Since the exceptional mechanical properties of polymer-crosslinked (X-) aerogels are ultimately traced to the conformal polymer coating, our basic hypothesis became that if that polymer itself could be made with the same nanostructure and interparticle connectivity as in X-aerogels, it should have similar mechanical properties. That hypothesis was demonstrated with extremely strong aerogels from almost all major classes of polymers, including polyureas, polyimides, polyamides (Kevlar[TM]-like), polybenzoxazines, poly(acrylonitrile-co-diacrylate), as well as polynorbornene and polydicyclopentadiene made via Ring Opening Metathesis Polymerization (ROMP). Apart from that wide array of new strong lightweight materials, at the fundamental level, ARO W911NF-10-1-0476 made apparent that:

(a) The nanostructure of polymeric aerogels may vary, seemingly arbitrarily, from nanoparticulate to nanofibrous, but consistently *nanofibrous structures are more resilient.* Thus, not only polymeric aerogels may be eventually the economically viable avenue to the general practical implementation of aerogels, but also *fibrous polymeric aerogels emerge as the most desirable candidates*; and,

(b) Irrespective of a nanoparticulate vs. a nanofibrous morphology, both types of nanostructures consist of about the same-size primary and secondary particles. Hence, controlling formation of nano-fibers over nano-globules becomes a task of understanding, controlling and directing the assembly of secondary nanoparticles into strings.

L. Dharani
Processing and Mechanical Characterization of Polyurea Aerogels

Polyurea (PUA) aerogels were proven to be mechanically strong, especially in terms of strength to weight. PUA aerogels can take extreme loads under compression; in the case of 0.31 g/cm^3 was able to support forty thousand times its own weight before yielding and over three million times its weight at the highest strain values. Results also indicate that polyurea aerogels are not particularly sensitive to various mid-range frequencies. The change in storage modulus across the tested range was minimal. The 0.17 g/cm^3 damped the oscillatory motion more effectively in tension than the other two densities. Compression simulations using PFC3D were completed using the PUA model. Simulations showed that the shear and normal stiffness of the particles were equivalent rather than a ratio as suggested by literature. From the available information PUA aerogels would be well suited to an application where low weigh, high stress, and high strain were necessary as long as loading only occurred once. Such applications could include impact-absorbing structures used in automobiles. If the manufacturing costs can be kept low, PUA aerogels could have a number of engineering applications.

J. Winiarz
Cost-Effective Synthesis of Vanadia Aerogels and Derivatives for Applications in Thermochromics, Energy Storage and Ballistics

We have successfully fabricated vanadium oxide (VO_x) aerogels using $VOCl_3$ instead of $VO(OPr)_3$, at a significantly reduced cost. Gels produced with this precursor have a nanoworm micromorphology identical to those fabricated using the alkoxide. Initial characterizations demonstrate that the wet gels are also much sturdier than alkoxide wet gels leading to improved processability. The gels can be crosslinked using Desmodur N-3200 bifunctional isocyanate to

produce mechanically strong X-aerogels. These gels can be used to form vanadium nitrite (VN) aerogels using aromatic isocyanate crosslinking and pyrolysis under NH_3. We have also modified this method to produce high-quality VO_2 films, which have potential application as a thermochromic coating for energy efficient windows. More recently vanadium oxide aerogels have been fabricated using V_2O_5 as a vanadium source, further lowering the cost. These gels were found to have particulate morphology and are also susceptible to isocyanate crosslinking. Finally, we have developed a facile hydrothermal method for synthesizing uniform $Li_\alpha V_6 O_{13}$ and $VO_2(B)$ nanoparticles which have application as Li-ion battery cathode materials.

Y. Xing
Flame Synthesis of VOx and ZnO Nanoparticles
The goal was to use a flame process to make metal oxide nanoparticles with unique morphology and to explore their conversion to hard nanoporous materials. Toward the goal we have accomplished synthesis of vanadium oxide nanoparticles and their conversion to nanoporous VC using a coating and pyrolysis process. We have also explored making ZnO nanorods in the flame reactor, which is a continuous process.

University of Missouri – Kansas City (Co-Lead Organization)

Z. Peng
Development and Self-Assembly of Multifunctional Inorganic-Polymer Hybrid Materials for Solar Energy Applications
The primary objectives of the original proposal are to develop various inorganic-polymer hybrid materials, study their self-assembly processes using innovative characterization techniques, and explore their potential applications as new multifunctional materials. During the three years under this grant support, we have made significant progress in a number of research fronts. For the inorganic component, we have demonstrated the convenient synthesis of various semiconducting nanoparticles and continued studying functionalized polyoxometalates (POMs). We have shown that surface charged nanoparticles in solutions can self-assemble into thermodynamically stable single-shell hollow nanovesicles. Such nanovesicle structures may find important applications as photocatalysts for solar water splitting and as traceable drug carriers. We have synthesized the first hybrid rod-coil diblock copolymers with POM clusters covalently attached to the coil block. We have shown that such hybrid diblock copolymers exhibit unique solution self-assembly behavior. We have demonstrated the photovoltaic properties of such POM-containing hybrids and identified areas for further improvement. We have synthesized new polycyclic aromatic compounds which can be solution processed into thin films which exhibit unusually high hole mobility. We have also shown that such molecules, when coated on the surface of nanofibers formed by electron acceptors, can behave as photoinduced electron donors and significantly enhance the photocurrent response of the nanofibers. We have designed new low band-gap donor-acceptor conjugated polymers and demonstrated their good solar cell performances. We have demonstrated that mechanical alloying can be used to prepare carbon nanodots which can be used as interfacial layer in hybrid solar cells with dramatically improved short circuit currents. We have also developed other conjugated systems including conjugated foldmers and dendrimers.

Oklahoma State University (Sub-Contractor)

F. Blum
Development and Study of Amine Sensors Based on Metal Nanoparticle-Doped Polyaniline
The major part of this work was in the development and understanding of sensors made in a one-step green process. We discovered that when aniline, water, a free radical oxidizer, and an acid dopant were irradiated with some form of moderate-energy radiation, polyaniline nanofibers

could be made. The addition of metal ions resulted in nanometal particles embedded in the polyaniline fibers. Using ultraviolet radiation and a drop of the precursor solution with metal particles on an interdigitated array allowed the easy production of sensors that were very sensitive to amines. Silver-containing sensors were the most sensitive. The response of the sensors to toluene and triethylamine were analyzed with a diffusion and surface adsorption model. In another system, the behavior of the surfactant, cetyltrimethylammonium bromide (CTAB), adsorbed on silica was analyzed with FTIR and calorimetry. The results were interpreted with a layered model. The first layer of CTAB on silica was rather disordered, followed by a more ordered bilayer, followed by layers that approach bulk-like (well ordered) structures.

Virginia Commonwealth University (Sub-Contractor)

M. Bertino
Regioselective Cross-Linking of Silica Aerogels with Magnesium Silicate Ceramics
The VCU team developed a fabrication method, which allows one to mechanically reinforce aerogels without compromising their porosity since the core retains the characteristics of native aerogels [1]. The reinforcement is ceramic in nature (mainly magnesium silicate) and it is stable at temperatures comparable to the densification temperature of silica aerogels (~900 ^{o}C), which are much higher than the temperatures (~200 ^{o}C) accessible to polymer-reinforced aerogels. Cross-linking depends on the presence of carbon in the aerogel structure. We obtained cross-linking only when carbonization conditions had been fulfilled, that is, PAN was used as a crosslinker, oxidized at 225 ^{o}C in air and then heated to the carbonization temperature of 850 ^{o}C. Masking allows one to reinforce only selected parts of aerogels and it could be employed to integrate aerogels into mechanical assemblies by reinforcing only the regions most subject to mechanical stress. Our results may also allow development of non-aerogel ceramic materials with anisotropic physical and chemical composition. In our process, chemical and physical properties are altered within the same monolith by introducing a catalyst (carbon in our case) for a solid-state reaction using conventional lithographic methods. The flexibility of lithography allows in principle to generate complicated patterns, which are not accessible to conventional methods of fabrication of anisotropic ceramics such as layering, bonding and generation of temperature and/or chemical gradients during processing.

Synthesis of Robust Nanoporous All-Polymer Aerogels as Multifunctional Materials for Acoustic and Thermal Insulation and Energy Absorption Applications

Professors Nicholas Leventis and Chariklia Sotiriou-Leventis

Department of Chemistry, MS&T

1. Introduction

Aerogels were invented in the 1930s in order to study the structure of wet-gels [1]. They are low-density, high porosity solids obtained by drying wet-gels under conditions that preserve their volume [2]. That usually involves converting and venting off the pore-filling solvent as a gas-like supercritical fluid (SCF). That process eliminates the surface tensions forces associated with evaporation that would cause collapse of the nanostructure. Quickly, aerogels became known as nanostructured solids with low-density (typically <0.2 g cm^{-3}) and high porosity (>80% v/v).

Owing to those properties, aerogels have some very attractive attributes, such as low thermal conductivity, high acoustic attenuation, and their mesoporous space can become host of functional guests with useful chemical, electrical, magnetic or optical properties [3]. Almost immediately, those attributes shifted attention from the original fundamental intent of their invention to applications. Thus, aerogels have been overlooked as a research tool by the soft matter community.

The most common kind of aerogels is based on silica, whose fragility, however, has limited applications mainly to space exploration (e.g., NASA's Stardust Program and Mars Rovers) [4]. By addressing the fragility issue, we have placed ourselves in a unique position to address the more general problem related to the fundamental composition of soft matter.

Specifically, the fragility of silica aerogels was rectified with polymer-crosslinked (X-) aerogels, whereas the surface functionality of pre-formed silica wet-gels plays the role of a chemical template that directs accumulation of a nano-thin conformal coating over the entire skeletal framework [5]. The polymer bridges covalently the skeletal nanoparticles and adds its chemical energy to the interparticle necks. For a nominal bulk-density increase by a factor of 2.5-3.0 (X-aerogels are still very low-density materials), the mechanical strength increases by a factor of 300. Applications unrelated to aerogels before (e.g., in armor) have become possible [6]. With carbonizable crosslinking polymers (e.g., polyacrylonitrile) X-aerogels have become starting materials for the synthesis of new porous materials (e.g., SiC aerogels via carbothermal reduction of the silica-core by the carbon shell [7]). According to unsolicited opinions, X-aerogels comprise a paradigm in the design of multi-functional nanostructured matter [8].

Along those efforts we reasoned that *since the exceptional mechanical properties of X-aerogels are ultimately traced to the conformal polymer coating, if that polymer itself could be made with the same nanostructure and interparticle connectivity as in X-aerogels, it should have similar mechanical properties.* In other words, **soft matter does not have to be weak**. That hypothesis may be considered counterintuitive, because X-aerogels are expected to include synergistic effects reminiscent of polymer-matrix composites [9], which aren't anticipated from pure polymers. Nevertheless, underlining the importance of the nanostructure, our hypothesis has been validated via this funding from ARO (W911NF-10-1-0476) with extremely strong aerogels from almost all major classes of polymers, including polyureas [10], polyimides [11], polyamides (Kevlar^{TM}-like) [12], polybenzoxazines [13], poly(acrylonitrile-co-diacrylate) [14], as well as polynorbornene and polydicyclopentadiene made via Ring Opening Metathesis Polymerization (ROMP) [15].

2. Results from ARO W911NF-10-1-0476

(a) Elucidation of the location of the polymer in X-aerogels

More commonly, inorganic aerogels may consist of clusters of nanoparticles (e.g., silica, Fig. 1A), and only rarely of nano"worms" (e.g., vanadia, Fig. 1C). In the cross-linking (X-) process, the innate surface –OH groups of *preformed* oxide wet-gels become anchoring cites for the accumulation of a poly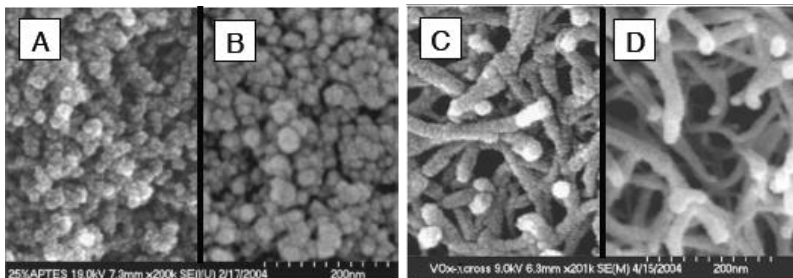mer coating, most commonly polyurea [5,6,16]. By introducing, other surface groups ($-NH_2$, styrene, free radical initiators, norbor-nene) numerous other polymers have been also used successfully (e.g., epoxies [17], polystyrene [18], polymethylmethacrylate [18,19], polyacrylonitrile [7], polynorbornene [20]). In addition to X-silica (Fig. 1B, [5-7,16-20]) and X-vanadia (Fig. 1D, [21]), the cross-linking method has been demonstrated with

Fig. 1. SEM of: A. a native (non-crosslinked) silica aerogel (0.19 g cm^{-3}; Π=89%); B. same aerogel crosslinked with polystyrene (0.48 g cm^3; Π=65%). C: Native vanadia aerogel (0.078 g cm^{-3}; Π=97%). D: Vanadia aerogel crosslinked with polyurea (0.42 g cm^{-3}; Π=67%). (Π: porosity as % v/v of empty space.)

~30 other oxide aerogels [22]. The polymer coating has been referred to as "conformal" meaning that it follows the contours of the inorganic backbone. However, the latter consists of a hierarchical network whereas primary nanoparticles form highly porous mass fractal assemblies referred to as secondary particles, which in turn form higher aggregates and so on. The exact location of the polymer in that nanostructure remained elusive, but was eventually resolved with ARO W911NF-10-1-0476.
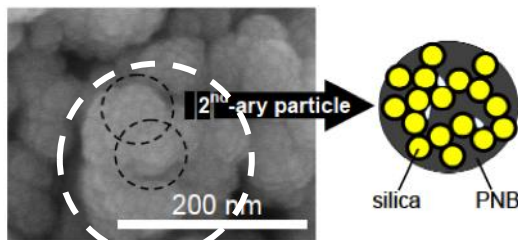
Fig 2. Polynorbornene (PNB)-crosslinked silica aerogels via ROMP. Yellow-filled circles: Primary particles. Black dashed circles: secondary particles. White dashed circle: network-forming aggregates. (The greatly improved mechanical properties are attributed to polymers confined within secondary particles, hence invisible by SEM [20].)

As it turns out (2012, [20]) with a judicious choice of the crosslinking polymer (polynorbornene), and a battery of methods relating the porous structure (via N_2-sorption and Hg-intrusion porosimetry) with: (a) the polymer molecular structure and density (via GPC, solids ^{13}C NMR and He pycnometry); (b) the fractal dimension of secondary particles (via SANS and SAXS); (c) the fractal dimension of particles forming the network (via rheology); and, (d) the bulk mechanical properties of the material, we concluded that polymer first coats primary particles, then fills 2nd-ary particles (Fig. 2), and most of the mechanical strength enhancement is obtained when the polymer starts spilling out into the fractal space of the next-level aggregates. Clearly, the role of the inorganic framework was just that of a templating agent for the polymer.

(b) All-polymer aerogels with the nanostructure of X-aerogels.
In addition to the conceptual challenge outlined in the Introduction, the practical advantage of all-polymer versus X-aerogels is their simplified one-step synthetic protocol for similar mechanical properties. For this, the three

design rules articulated via ARO W911NF-10-1-0476 are [14]: (a) work under conditions that induce early phase separation of the developing polymer into the tiniest primary colloidal nanoparticles possible; (b) the most efficient way to do "(a)" is with small-molecule soluble multifunctional monomers that produce crosslinked, highly-insoluble polymers; and, (c) classic (industrial) methods for polymer synthesis, which frequently rely on oligomeric precursors, may not be the most suitable for aerogel synthesis. Rules (a) and (b) ensure that phase-separated nanoparticles have high surface functional group density to promote extensive interparticle crosslinking. That principle works well even with *virtual* primary particles (micelles: e.g., emulsion gelation of acrylonitrile in water [14]). Next, we review representative systems that have emerged via ARO W911NF-10-1-0476.

b.1 **_Polyurea (PUA) aerogels._**   Polyurea (PUA) aerogels were synthesized via Eq.s 1 and 2 from an aliphatic (Desmodur N3300A), or an aromatic (Desmodur RE) triisocyanate [10]. Both mono-

$$O=C=N-R-N=C=O \ + \ 2\,H_2O \ \xrightarrow{Et_3N} \ H_2N-R-NH_2 \ + \ 2\,CO_2 \qquad (1)$$

$$O=C=N-R-N=C=O \ + \ H_2N-R-NH_2 \ \longrightarrow O=C=N-R-NH(CO)NH-R-NH_2 \quad (2)$$

[Et$_3$N: triethylamine (catalyst)]

Desmodur N3300A   Desmodur RE
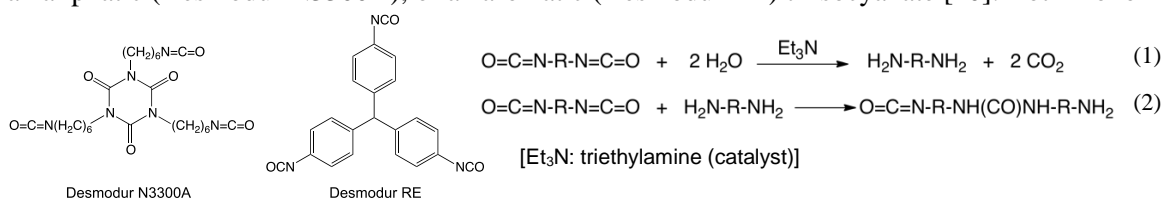
mers have been courtesy of Bayer Corp. USA. They are supplied in bulk quantities, yet they are pure compounds (for full characterization see Ref [10a]). Eq.s 1 and 2 are rarely used for the synthesis of bulk polyureas; they are typically involved in the environmental curing of PUA films, or as a foaming mechanism for polyurethanes [23]. The main advantage of the Eq.s 1 & 2 route is that it bypasses polyamines [24,25], which can be expensive, and replaces them with water.

The bulk density of PUA aerogels has been varied over a wide range (0.016-0.6 g cm^{-3}), and
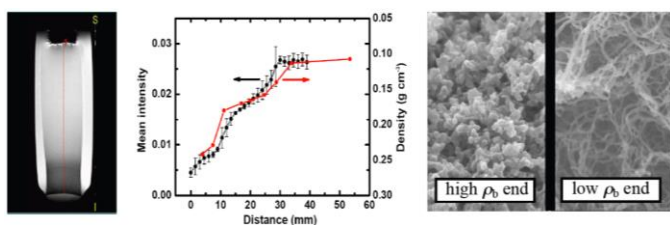
Fig. 3. Density-gradient PUA aerogel monoliths from Desmodur N3300A. <u>Left</u>: magnetic resonance imaging (MRI) of a H$_2$O-filled sample; high-density end at the bottom. <u>Middle</u>: Density variation by MRI and by direct measurement. <u>Right</u>: SEM: high-density end, particulate (*Π*=54%) low-density end, fibrous (*Π*=94%).

although the chemical composition remains the same, the nanostructure varies: at lower-densities is fibrous, turning particulate as the density increases. This is demonstrated in Fig. 3 with a variable-density monolith. Small angle neutron scattering (SANS) has shown that both morphologies consist of almost identical spherical primary particles (R_G~3-10 nm), which assemble into mass-fractal secondary particles that in turn form fibers or higher (mass or surface) fractal agglomerates [10a]. The specific energy absorption under quasi-static compression of ~0.6 g cm^{-3} samples was 90 J g^{-1} at 23 ^{o}C, and 55 J g^{-1} at -173 ^{o}C, reaching compressive strains of over 90%. Under tension, fibrous low-density samples (<u>b</u> and <u>c</u>, Fig. 4) can tolerate twice as much strain as their higher-density counterparts (<u>a</u>), so that as the density decreases, the total energy absorption remains about the same, or even improves (sample <u>b</u>). These results underline the practical utility of fibrous nanostructures.
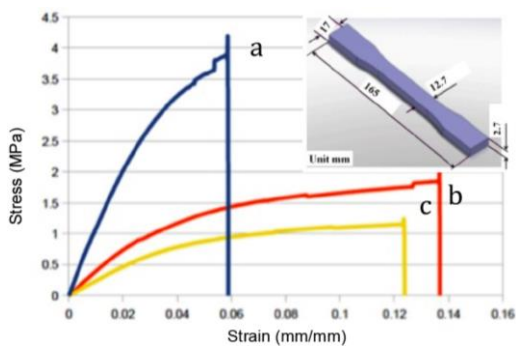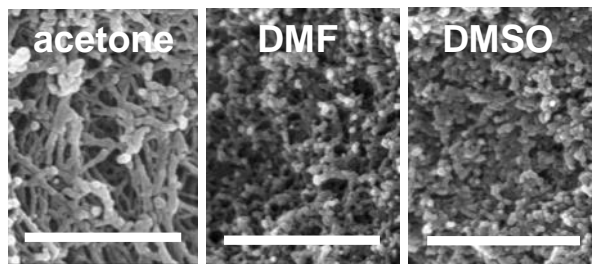
Fig. 4. Tensile testing of PUA aerogels from Desmodur N3300A at 23 $^{\circ}$C: (a) 0.31g cm^{-3} (particulate); (b) 0.17 g cm^{-3} (fibrous); (c) 0.12 g cm^{-3} (also fibrous). <u>Inset</u>: dog-bone sample used for testing. (***Unpublished results in collaboration with co-PI Prpfessor Dharani – see below.***)

ρ_b=0.13 g cm^{-3}	ρ_b=0.11 g cm^{-3}	ρ_b=0.13 g cm^{-3}
Π = 90% v/v	Π = 91% v/v	Π = 89% v/v
σ = 169 m^2 g^{-1}	σ = 307 m^2 g^{-1}	σ = 280 m^2 g^{-1}

Fig. 5. SEM of PUA aerogels at similar bulk densities (ρ_b), prepared with Desmodur N3300A in 3 different solvents. Notice the change in morphology from fibrous to particulate. All scale bars at 1 μm. (Π: porosity. σ: surface area via the BET method (N$_2$ sorption) [26].

In the context of this proposal, we first reasoned that the effect of varying the monomer concentration (Fig. 3) operates through a change in the dielectric properties of the medium (solvent + monomer). Indeed, moving from acetone (polarity index, PI=5.08) to DMSO (PI=8.02), nanoparticles were favored at all densities (Fig. 5) [26]. In intermediate-polarity DMF (PI=6.70), we observed an intermediate morphology with short strings of nanoparticles (Fig. 5). Curiously, however, moving to even more polar CH$_3$CN (PI=8.80), the nanostructure (Fig. 6) deviates significantly from all those in Fig. 5: we observe cocoon-like objects entrapped in fiber web, and the material is extremely flexible and superhydrophobic (water contact angle, θ=150.0°; dense PUA itself is hydrophilic with θ=69.1°) [26]. Inexpensive access to texture-induced superhydrophobicity is technologically important (self cleaning surfaces, environmental remediation etc.) [27].
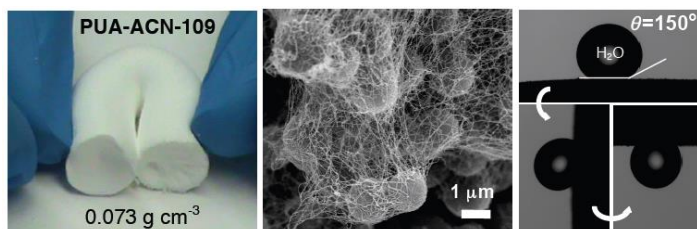
Fig. 6. A flexible, monolithic, super-hydrophobic PUA aerogel made with Desmodur N3300A in acetonitrile (ACN). (Note: the water droplet does not run off by turning the substrate upside-down: Petal effect super-hydrophobicity. [26])

b.2 Polyurethane aerogels. Allegedly, polyurethane (PU) aerogels based on industrial oligomeric diisocyanates and diols with 1,4-diazabicyclo[2.2.2]octane (DABCO) as catalyst are known [28]. However, many of those materials may not have been polyurethanes at all, but rather poly(isocyanurates) resulting from trimerization of –N=C=O (DABCO is a well-known trimerization catalyst [29]) with some allophanate crosslinking: it is rather improbable for linear polyurethanes from highly soluble oligomers to form very strong gels. Indeed, the <u>non-catalyzed</u> reaction of Desmodur N3200 diisocyanate and diol end-capped poly(1,4-butylene adipate) (M_n~1,000, Aldrich) [5a], or PEO (600<M_n<3000) yields materials that collapse upon drying, even with SCF CO$_2$, setting the stage against linear polymer gels. Considering all of the above, our recently (2013) reported studies of PU aerogels [30] used: (a) dibutyl tin dilaurate as a Lewis acid catalyst known to induce only polyurethane formation [31]; and, (b) readily available *small*

molecule multifunctional monomers. Our triisocyanates were Desmodur N3300A and Desmodur RE, and the small molecule aromatic alcohols included:

phloroglucinol
(POL, n=3, r=3)

recorcinol
(RES, n=2, r=2)

1,1,1-tris(4-hydroxyphenyl) ethane
(HPE, n=3, r=1)

R: SO$_2$; 4,4'-sulfonyldiphenol
(SPD, n=2, r=1)

R: C=O; 4,4'-dihydroxybenzophenone
(DHB, n=2, r=1)

R: C(CH$_3$)$_2$; 4,4'-isopropylidenediphenol
(BPA, n=2, r=2)
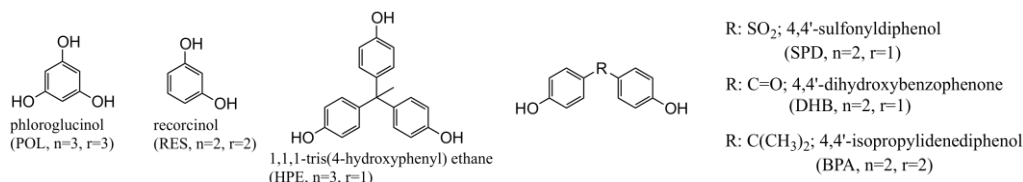
Satisfactory aerogels in terms of high porosities, surface areas and mechanical strength were obtained only with rigid Desmodur RE. All gelations were run in acetone, with a few controls in THF and DMSO. Those materials could vary from extremely robust (compressive modulus~650 MPa, specific energy absorption >100 J g^{-1}) to rubber-like flexible foams (Fig. 7). Flexible PU aerogels consisted of larger particles. A very strong correlation was found between mechanical strength and *n+r*, (number of OH groups per polyol + OH groups per aromatic ring) in support of our hypothesis that the functional group density at the molecular level translates into a higher functional group density on nanoparticles, resulting to more efficient interparticle crosslinking (the latter was investigated and confirmed via a top-down characterization protocol from bulk modulus and solid thermal conduction data). Morphologically, the similarity between X-silica aerogels (Fig. 1B) and the rigid variety of the PU aerogels is striking.
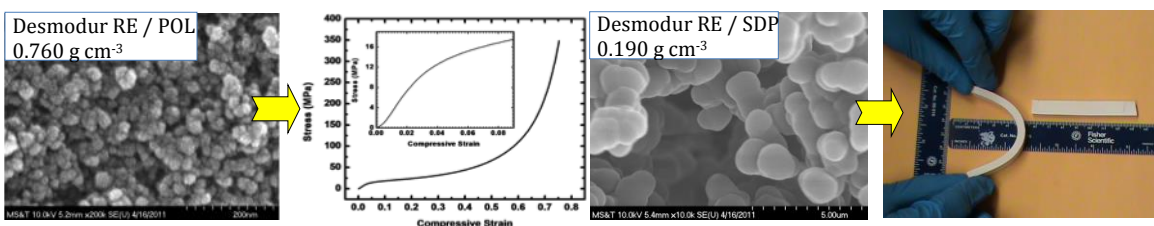
Fig. 7. Two types of polyurethane aerogels ranging from super-rigid (left) to flexible (right), both synthesized with Desmodur RE triisocyanate and two small-molecule aromatic alcohols (see above).

*b.3 **Polyimide aerogels**.* Polyimides are used in high-T applications and are synthesized commercially by two methods: (a) condensation (>190 °C) of aromatic dianhydrides and amines (the DuPont route, e.g., Kapton^{TM}) [32], or (b) crosslinking (>300 °C) of norbornene end-capped imide oligomers (the PMR route; PMR: polymerization of monomer reactants) [33,34].

Scheme 1. Polyimide through the isocyanate (PI-ISO) and the amine (PI-AMN) routes
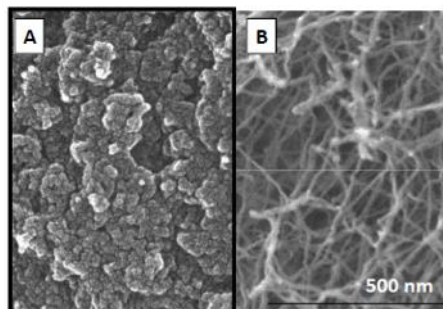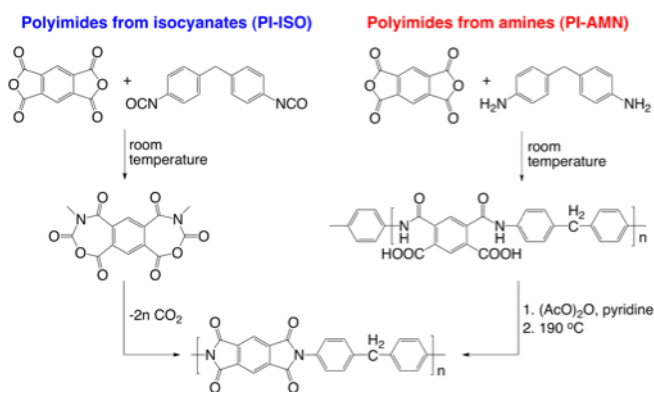
Fig. 8. (A) PI-AMN (ρ_b=0.186 g cm^{-3}, Π=87% v/v, ρ_s=1.453 g cm^{-3}, BET surface area=431 m^2 g^{-1}). (B) PI-ISO (ρ_b=0.090 g cm^{-3} Π=94% v/v, ρ_s=1.473 g cm^{-3}, BET surface area=315 m^2 g^{-1}) [11a,11b].

9

Polyimide aerogels via the DuPont route were reported in a 2006 US patent [35]. We duplicated those results and in parallel we developed a *room-temperature* alternative method via the underutilized reaction of aromatic dianhydrides with multifunctional isocyanates [36]. Scheme 1 compares the two methods and emphasizes that both yield chemically identical products [11a,11b]. SANS has shown that materials synthesized in NMP via either route consist of similar size primary (1°) and secondary (2°) particles (radii or gyration, R_G, for primary and secondary particles of polyimide aerogels from the isocyanate/amine route: 4.7/5.8 nm and 35/42 nm, respectively). SEM, however, (Fig. 8) shows that 2°-particles assemble into fibers in the isocyanate route, and into globular aggregates in the amine route. The difference was attributed to the rigidity of the 7-membered ring intermediate in the isocyanate route (Scheme 1) [11a,11b].

More recent studies (2013) with pyromellitic dianhydride and Desmodur RE triisocyanate yielded strings of particles turning to clusters of particles at higher concentration sols [11c]. Most importantly, those materials include intrinsic microporosity, which was confirmed via simulations. Using the experimental XRD pattern, the particle size and the skeletal density of the polymer as gauges for the fidelity of the simulations, we found out that primary particles are not single polymer entities, but rather H-bonded or van der Waals assemblies of oligomers, stacked together, then packed together and eventually coiled up to maximize those non-covalent interactions between oligomers in different stacks. Fig. 9 uses two different polyimides to demonstrate the ability of that approach to reproduce both the XRD pattern and the micropore size by stacking and packing of second-generation dendritic oligomers [11c].
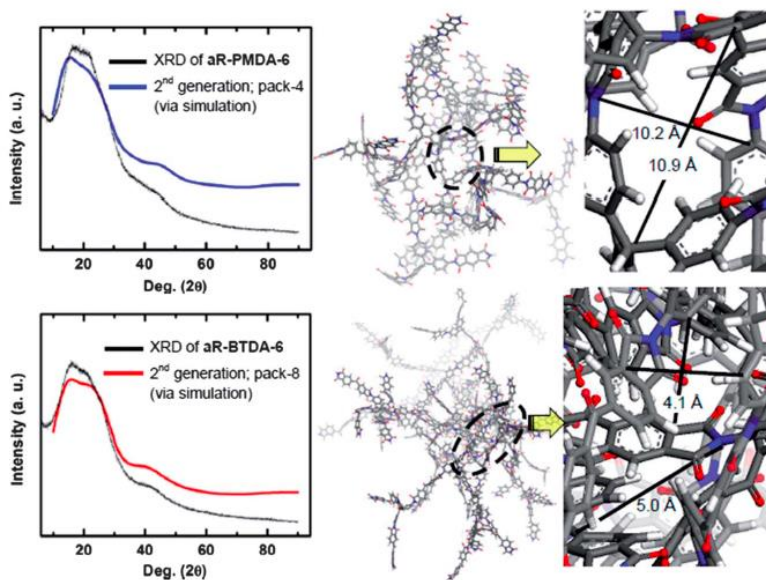
Fig. 9. Left: best-match of simulated XRD patterns with the experimental data as indicated. (**"Pack-x"** refers to the number of hyperbranched polyimide oligomers introduced in the molecular dynamics simulations. Middle: structures corresponding to the simulated XRDs on the left. Right: magnification of the voids enclosed by dashed ovals in middle.

b.4 ROMP-derived aerogels. We entered this area by reasoning that ROPM should be a viable low-temperature alternative to the high-temperature PMR route to polymides. With ARO funding, that conjecture has been fully justified (see Fig. 10 [37]), and the expertise was applied to X-silica aerogels crosslinked with polynorbornene leading to mapping topologically the location of the polymer on the silica nanostructure (Fig. 2) [20]. About concurrently with our report on the ROMP alternative to PMR polymides [37], Aspen Aerogels reported on polydicyclopentadiene (pDCPD) aerogels [38]. This area is picking momentum for strong lightweight materials [39], perhaps because of Grubbs' intriguing photograph in his Nobel lecture showing 9 mm bullets
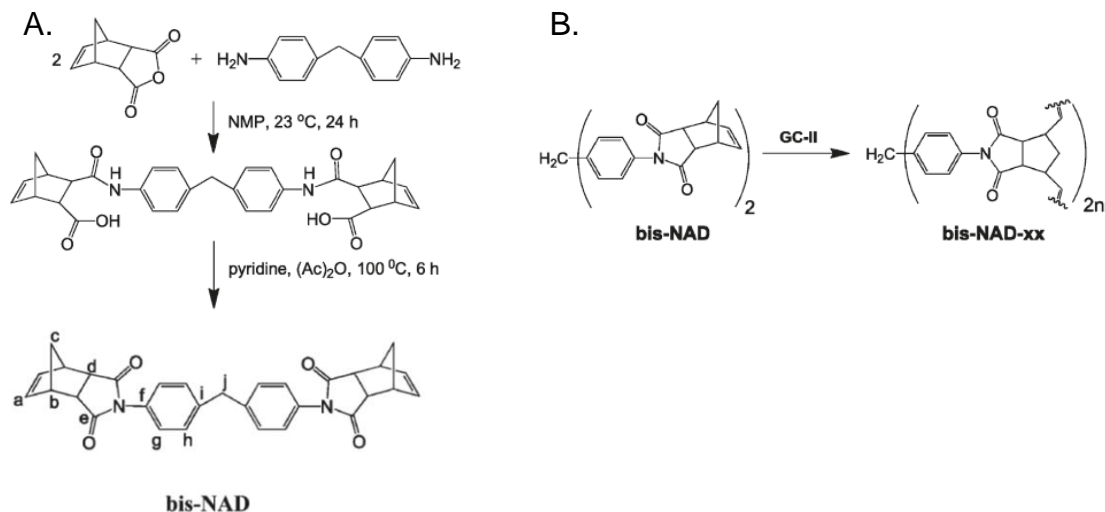
Fig. 10. (A) Synthesis of **bis-NAD** diimide monomer. (B) ROMP polymerization of bis-NAD. The polymer (**bis-NAD-xx**) composes the skeletal framework of the aerogels. (GC-II: second generation Grubgs' catalyst.
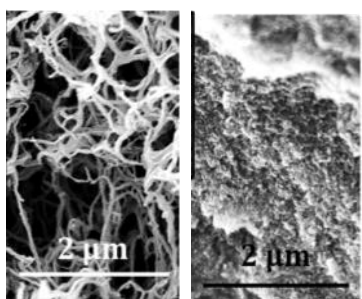

Fig. 11. pDCPD aerogels. Left: ρ_b = 0.084 g cm^{-3}, σ = 207 m^2 g^{-1}. SAXS diameters: 1° particles = 12.8 nm; 2° particles = 148 nm. Right: ρ_b = 0.55 g cm^{-3}, σ = 193 m^2 g^{-1}. SAXS diameters: 1° particles = 39.6 nm; 2° particles = 123 nm. (***Unpublished results.***)

embedded in a dense pDCPD polymer block [40]. Our attempts to synthesize pDCPD aerogels by duplicating literature procedures yielded *severely* deformed monoliths. That issue was alleviated by free radical polymerization of methylmethacrylate (MMA) in the pores, engaging some of the double bonds of the ROMP-derived polymer, and yielding polyMMA (PMMA) grafted to the network. Those results were presented at the 242nd ACS meeting in Denver, CO (August 2011) - the paper was selected for the Sci-Mix [15a]. Detailed structural analysis revealed that PMMA prevents deformation by filling and rigidizing secondary pDCPD nanoparticles in analogy to polynorbornene filling silica (refer to Fig. 2) [15b]. However, most importantly for this proposal, in analogy to PUA aerogels, the pDCPD network may consist of fibers (at lower densities) or particles (at higher ones), but both morphologies share the same hierarchical structure of primary/secondary particles (Fig. 11 - legend).

Other systems include polyamide (Kevlar^{TM}-like) aerogels [12] from carboxylic acids and isocyanates [41], and "green" polyacrylonitrile aerogels via emulsion gelation in water [14]. The latter system tested the novel concept of creating and using micelles as virtual nanoparticles. Since polyacrylonitrile is the main industrial source of carbon (graphite) fiber, polyacrylonitrile aerogels were pyrolyzed at 2,300 oC and were converted to graphite, thus demonstrating the first graphitic aerogels. Those materials turn out to be monolithic, very robust and electrically conducting, as expected. Surprisingly, however, we also discovered that graphitic aerogels include rod-like microstructures, which are quite rare and have been observed in some natural graphite from only a couple of mines around the world. A representative example of those rod-like graphitic structures is shown in Fig. 12. Similar structures have been observed with other kinds of carbonizable aerogels (e.g., certain polyureas, polyimides, polyamides, polybenzoxazines) and a mechanism is being worked out.
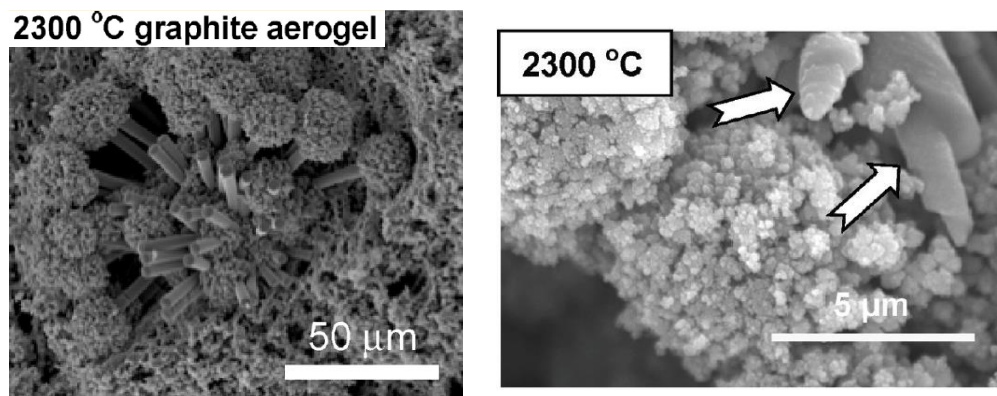
Fig. 12. Rod-like structures in graphitic aerogels from pyrolysis at 2,300 $^{\circ}$C of polyacrylonitrile aerogels

3. Summary

Apart from a wide array of new strong lightweight materials based on almost all polymeric classes and covered by numerous patent applications, at the fundamental level, ARO W911NF-10-1-0476 made apparent that:

(a) The nanostructure of polymeric aerogels may vary, seemingly arbitrarily, from nanoparticulate to nanofibrous, but consistently *nanofibrous structures are more resilient.* Thus, not only polymeric aerogels may be eventually the economically viable avenue to the general practical implementation of aerogels, but also *fibrous polymeric aerogels emerge as the most desirable candidates*; and,

(b) Irrespective of a nanoparticulate vs. a nanofibrous morphology, both types of nanostructures consist of about the same-size primary and secondary particles. Hence, controlling formation of nano-fibers over nano-globules becomes a task of understanding, controlling and directing the assembly of secondary nanoparticles into strings.

4. References

[1]   (a) Kistler, S. S. "Coherent Expanded Aerogels and Gellies," *Nature* **1931**, *127*, 3211.

(b) Kistler, S. S. "Coherent Expanded-Aerogels," *J. Phys. Chem.* **1932**, *36*, 52-63.

[2]   (a) Gesser, H. D.; Goswami, P. C. "Aerogels and Related Porous Materials," *Chem. Rev.* **1989**, *89*, 765-788.

(b) Fricke, J. "Aerogels," *Sci. Am.* **1998**, *258*, 92-97.

[3]   (a) Morris, C. A.; Anderson, M. L.; Stroud, R. M.; Merzbacher, C. I.; Rolison, D. R. "Silica Sol as a Nanoglue: Flexible Synthesis of Composite Aerogels," *Science* **1999**, *284*, 622-624.

(b) Pierre, A. C.; Pajong, G. M. "Chemistry of Aerogels and Their Applications," *Chem. Rev.* **2002**, *102*, 4243-4265.

(c) Rolison, D. "Catalytic Nanoarchitectures - The Importance of Nothing and the Unimportance of Periodicity," *Science* **2003**, *299*, 1698-1701.

(d) "Aerogels Handbook, Advances in Sol-Gel Derived Materials and Technologies," Aegerter, M.; Leventis, N.; Koebel, M., Eds.; Springer: New York, **2011**.

[4]   Jones, S. M.; Sakamoto, J. "Applications of Aerogels in Space Exploration," in "Aerogels Handbook, Advances in Sol-Gel Derived Materials and Technologies," Aegerter, M.; Leventis, N.; Koebel, M., Eds.; Springer: New York, **2011**, Chapter 32, pp 721-746.

[5]   (a) Leventis, N.; Sotiriou-Leventis, C.; Zhang, G.; Rawashdeh, A.-M. M. "Nano Engineering Strong Silica Aerogels," *NanoLetters* **2002**, *2,* 957-960.

      (b) Zhang, G.; Dass, A.; Rawashdeh, A.-M. M.; Thomas, J.; Counsil, J. A.; Sotiriou-Leventis, C.; Fabrizio, E. F.; Ilhan, F.; Vassilaras, P.; Scheiman, D. A.; McCorkle, L.; Palczer, A.; Johnston, J. C.; Meador, M. A. B.; Leventis, N. "Isocyanate-Crosslinked Silica Aerogel Monoliths: Preparation and Characterization," *J. Non-Cryst. Solids* **2004**, *350*, 152-164.

      (c) Leventis, N. "Three Dimensional Core-Shell Superstructures: Mechanically Strong Aerogels," *Acc. Chem. Res.* **2007**, *40*, 874-884.

[6]   (a) Leventis, N.; Lu, H. "Polymer Crosslinked Aerogels," in "Aerogels Handbook, Advances in Sol-Gel Derived Materials and Technologies," Aegerter, M.; Leventis, N.; Koebel, M. Eds.; Springer: New York, **2011**, pp 251-285.

      (b) Luo, H.; Lu, H.; Leventis, N. "Mechanical Characterization of Aerogels," in "Aerogels Handbook, Advances in Sol-Gel Derived Materials and Technologies," Aegerter, M.; Leventis, N.; Koebel, M. Eds.; Springer: New York, **2011**, pp 499-535.

[7]   (a) Leventis, N.; Sadekar, A.; Chandrasekaran, N.; Sotiriou-Leventis, C. "Click Synthesis of Monolithic Silicon Carbide Aerogels from Polyacrylonitrile-Coated 3D Silica Networks," *Chem. Mater.* **2010**, *22*, 2790-2803.

      (b) Sadekar, A. G.; Chandrasekaran, N.; Sotiriou-Leventis, C.; Leventis, N. "Porous Monolithic Silicon Carbide Aerogels from Polyacrylonitrile-Coated 3D Silica Networks," *PMSE Preprints*, **2010**, *103*, 188-190.

[8]   See for example:
      (a) Eychmüller, A. "Aerogels for Semiconductor Nanomaterials," *Angew. Chem. Int. Ed.* **2005**, *44*, 4839-4841.

      (b) "Strong and Flexible Aerogels" at http://www.aerogel.org/?p=1058 (11/06/2013)

      (c) Aegerter, M. A.; Leventis, N.; Koebel M. M. "Concluding Remarks," in *Aerogels Handbook, Advanced in Sol-Gel Derived Materials and Technologies*, Aegerter, M. A.; Leventis, N.; Koebel M. M. Eds., Springer: New York, NY, 2011, pp 891-892.

[9]   (a) Balazs, A. C.; Emrick, T.; Russell, T. P. "Nanoparticle Polymer Composites: Where Two Small Worlds Meet," *Science* **2006**, *314*, 1107−1110.

      (b) Winey, K. I.; Vaia, R. A. "Polymer Nanocomposites," *MRS Bull.* **2007**, *32*, 314-322.

      (c) Thayer, A. M. "Nanomaterials," *Chem. & Eng. News*, Cover Story, 09-01-2003, p 15.

[10] (a) Leventis, N.; Sotiriou-Leventis, C.; Chandrasekaran, N.; Mulik, S.; Larimore, Z. J.; Lu, H.; Churu, G.; Mang, J. T. "Multifunctional Polyurea Aerogels from Isocyanates and Water. A Structure-Property Case Study," *Chem. Mater.* **2010**, *22*, 6692-6710.

(b) Chardrasekaran, N.; Mulik, S.; Larimore, Z.; Churu, G.; Lu, H.; Sotiriou-Leventis, C.; Leventis, N. "Efficient One-Step Synthesis of Mechanically Strong, Flame Retardant Polyurea Aerogels," *Polymer Preprints* **2010**, *51*, 334-335.

(c) Leventis, N.; Sotiriou-Leventis, C.; Chandrasekaran, N.; Mulik, S.; Chidambareswarapattar, C.; Sadekar, A.; Mohite, D.; Mahadik, S. S.; Larimore, Z. J.; Lu, H.; Churu, G.; Mang, J. T. "Isocyanate-Derived Organic Aerogels: Polyureas, Polyimides, Polyamides," *MRS Proceedings* **2011**, *1306*, mrsf10-1306-bb03-01, DOI: 10.1557/opl.2011.90.

(d) Bian, Q.; Chen, S.; Kim, B.-T.; Leventis, N.; Lu, H.; Chang, Z.; Lei, S. "Micromachining of Polyurea Aerogel Using Femtosecond Laser Pulses," *J. Non-Cryst. Solids* **2011**, *357*, 186-193.

[11] (a) Chidambareswarapattar, C.; Larimore, Z.; Sotiriou-Leventis, C.; Mang, J. T.; Leventis, N. "One-Step Room-Temperature Synthesis of Fibrous Polyimide Aerogels from Anhydrides and Isocyanates and Conversion to Isomorphic Carbons," *J. Mater. Chem.* **2010**, *20*, 9666-9678.

(b) Chidambareswarapattar, C.; Larimore, Z.; Sotiriou-Leventis, C.; Leventis, N. "Mechanically Strong Nanoporous Polyimides (Aerogels) from Anhydrides and Isocyanates: A Structure-Property Study," *PMSE* **2012**, *106*, 193-194.

(c) Chidambareswarapattar, C.; Xu, L.; Sotiriou-Leventis, C.; Leventis, N. "Robust Monolithic Multiscale Nanoporous Polyimides and Conversion to Isomorphic Carbons," *RSC Advances* **2013**, *3*, 26459-26469.

[12] (a) Leventis, N.; Chidambareswarapattar, C.; Mohite, D. P.; Larimore, Z. J.; Lu, H.; Sotiriou-Leventis, C. "Multifunctional Porous Aramids (Aerogels) by Efficient Reaction of Carboxylic Acids and Isocyanates," *J. Mater. Chem.* **2011**, *21*, 11981–11986.

(b) Chidambareswarapattar, C.; Mohite, D. P.; Larimore, Z. J.; Lu, H.; Sotiriou-Leventis, C.; Leventis, N. "One Pot Synthesis of Multifunctional Aramid Aerogels," *MRS Proceedings* (mrsf11-1403-v17-36) **2012**, Vol.: *1403*, pp. 1-6 (DOI: 10.1557/opl.2012.389).

[13] (a) Mahadik-Khanolkar, S.; Wisner, C.; Churu, G.; Lu, H.; Leventis, N.; Sotiriou-Leventis, C. "Polybenzoxazine Aerogels: Synthesis, Characterization and Conversion to Carbon and Graphite Aerogels," *PMSE Preprints* **2013**, *108*, 43-44.

(b) Mahadik-Khanolkar, S.; Donthula, S.; Sotiriou-Leventis, C.; Leventis, N. "Polybenzoxazine Aerogels. 1. High-Yield Room-Temperature Acid-Catalyzed Synthesis of Robust Monoliths, Oxidative Aromatization and Conversion to Microporous Carbons," *Chem. Mater.* **2014**, *26*, 1303-1317.

(c) Mahadik-Khanolkar, S.; Donthula, S.; Bang, A.; Wisner, C.; Sotiriou-Leventis, C.;

Leventis, N. "Polybenzoxazine Aerogels. 2. Interpenetrating Networks with Iron Oxide and the Carbothermal Synthesis of Highly Porous Monolithic Pure Iron(0) Aerogels as Energetic Materials," *Chem. Mater.* **2014**, *26*, 1318-1331.

[14]   Sadekar, A. G.; Mahadik, S. S.; Bang, A. N.; Larimore, Z. J.; Wisner, C. A.; Bertino, M. F.; Mang, J. T.; Sotiriou-Leventis, C.; Leventis, N. "Green Aerogels and Porous Carbons by Emulsion Gelation of Acrylonitrile," *Chem. Mater.* **2012**, *24*, 26-47.

[15]   (a) Mohite, D.; Larimore, Z.; Sotiriou-Leventis, C.; Leventis, N. "Polydicyclopentadiene Aerogels Grafted with Polymethylmethacrylate," *PMSE Preprints* **2011**, *105*, 358-360.

   (b) Mohite, D. P.; Mahadik-Khanolkar, S.; Luo, H.; Lu, H.; Sotiriou-Leventis, C.; Leventis, N. "Polydicyclopentadiene Aerogels Grafted with PMMA: I. Molecular and Interparticle Crosslinking," D. P. Mohite, S. Mahadik-Khanolkar, H. Luo, H. Lu, C. Sotiriou-Leventis, N. Leventis *Soft Matter* **2013**, *9*, 1516-1530.

   (c) Mohite, D. P.; Mahadik-Khanolkar, S.; Luo, H.; Lu, H.; Sotiriou-Leventis, C.; Leventis, N. "Polydicyclopentadiene Aerogels Grafted with PMMA: II. Nanoscopic Characterization and Origin of Macroscopic Deformation," *Soft Matter* **2013**, *9*, 1531-1539.

[16]   (a) Katti, A.; Shimpi, N.; Roy, S.; Lu, H.; Fabrizio, E. F.; Dass, A.; Capadona, L. A.; Leventis, N. "Chemical, Physical and Mechanical Characterization of Isocyanate-Crosslinked Amine-Modified Silica Aerogels," *Chem. Mater.* **2006**, *18*, 285-296.

   (b) Meador, M. A. B.; Capadona, L. A.; MacCorkle, L.; Papadopoulos, D. S.; Leventis, N. "Structure-Property Relationships in Porous 3D Nanostructures as a Function of Preparation Conditions: Isocyanate Cross-Linked Silica Aerogels," *Chem. Mater.* **2007**, *19*, 2247-2260.

   (c) Capadona, L.; Meador, M. A. B.; Alunni, A.; Fabrizio, E. F.; Vassilaras, P.; Leventis, N. "Flexible, Low-Density Polymer Crosslinked Silica Aerogels," *Polymer* **2006**, *47*, 5754-5761.

   (d) Leventis, N.; Mulik, S.; Sotiriou-Leventis, C. "Macroporous Electrically Conducting Carbon Networks by Pyrolysis of Isocyanate Cross-Linked Resorcinol-Formaldehyde Aerogels," *Chem. Mater.* **2008**, *20*, 6985-6997.

   (e) Yin, W.; Venkitachalam, S. M.; Jarett, E.; Staggs, S.; Leventis, N.; Lu, H.; Rubenstein, D. A. "Biocompatibility of Surfactant-Templated Polyurea-Nanoencapsulated Macroporous Silica Aerogels with Plasma and Endothelial Cells," *J. Biomed. Mater. Res. A* **2010**, *92A*, 1431-1439.

   (f) Sabri, F.; Leventis, N.; Hoskins, J.; Schuerger, A. C.; Sinden-Redding, M.; Britt, D.; Duran, R. A. "Spectroscopic Evaluation of Polyurea Crosslinked Aerogels, as a Substitute for RTV-based Chromatic Calibration Targets for Spacecraft," *Ad. Space Res.* **2011**, *47*, 419-427.

(g) Sabri, F.; Cole, J. A.; Scarborough, M. C.; Leventis, N. "Investigation of Polyurea-Crosslinked Silica Aerogels as a Neuronal Scaffold: A Pilot Study," *PLoS One* **2012**, *7(3)*, e33242.

[17]   Meador, M. A. B.; Fabrizio, E. F.; Ilhan, F.; Dass, A.; Zhang, G.; Vassilaras, P.; Johnston, J. C.; Leventis, N. "Crosslinking Amine-Modified Silica Aerogels With Epoxies: Mechanically Strong Lightweight Porous Materials," *Chem. Mater.* **2005**, *17*, 1085-1098.

[18]   Ilhan, U. F.; Fabrizio, E. F.; McCorkle, L.; Scheiman, D.; Dass, A.: Palczer, A.; Meador, M. A. B.; Leventis, N. "Hydrophobic Monolithic Aerogels by Nanocasting Polystyrene on Amine-Modified Silica," *J. Mater. Chem.* **2006**, *16*, 3046-3054.

[19]   Mulik, S.; Sotiriou-Leventis, C.; Churu, G.; Lu, H.; Leventis, N. "Crosslinking 3D Assemblies of Nanoparticles into Mechanically Strong Aerogels by Surface-Initiated Free Radical Polymerization," *Chem. Mater.* **2008**, *20,* 5035-5046.

[20]   (a) Mohite, D. P.; Larimore, Z. J.; Lu, H.; Mang, J. T.; Sotiriou-Leventis, C.; Leventis, N. "Monolithic Hierarchical Fractal Assemblies of Silica Nanoparticles Cross-Linked with Polynorbornene via ROMP: A Structure-Property Correlation from Molecular to Bulk through Nano," *Chem. Mater.* **2012**, *24*, 3434-3448.

(b) Mohite, D.; Larimore, Z.; Leventis, N.; Sotiriou-Leventis, C. "Strong Silica Aerogels Crosslinked with Polynorbornene via Ring Opening Metathesis Polymerization (ROMP)," *Polymer Preprints* **2010**, *51*, 469-470.

[21]   (a) Leventis, N.; Sotiriou-Leventis, C.; Mulik, S.; Dass, A.; Schnobrich, J.; Hobbs, A.; Fabrizio, E. F.; Luo, H.; Churu, G.; Zhang, Y.; Lu, H. "Polymer Nanoencapsulated Mesoporous Vanadia With Unusual Ductility at Cryogenic Temperatures," *J. Mater. Chem.* **2008**, *18*, 2475-2482.

(b) Luo, H.; Churu, G.; Schnobrich, J.; Hobbs, A.; Fabrizio, E. F.; Dass, A.; Mulik, S.; Sotiriou-Leventis, C.; Lu, H.; Leventis, N. "Physical, Chemical and Mechanical Characterization of Isocyanate-Crosslinked Vanadia Aerogels," *J. Sol-Gel Sci. Technol.* **2008**, *48*, 113-134.

[22]   (a) Leventis, N.; Vassilaras, P.; Fabrizio, E. F.; Dass, A. "Polymer Nanoencapsulated Rare Earth Aerogels: Chemically Complex but Stoichiometrically Similar Core-Shell Superstructures with Skeletal Properties of Pure Compounds," *J. Mater. Chem.* **2007**, *17*, 1502-1508.

(b) Leventis, N.; Chandrasekaran, N.; Sotiriou-Leventis, C.; Mumtaz, A. "Smelting in the Age of Nano: Iron Aerogels," *J. Mater. Chem.* **2009**, *19*, 63-65.

(c) Leventis, N.; Chandrasekaran, N.; Sadekar, A. G.; Sotiriou-Leventis, C.; Lu, H. "One-Pot Synthesis of Interpenetrating Inorganic/Organic Networks of CuO/Resorcinol-Formaldehyde Aerogels: Nanostructured Energetic Materials," *J. Am. Chem. Soc.* **2009**, *131*, 4576-4577.

(d) Leventis, N.; Chandrasekaran, N.; Sadekar, A. G.; Mulik, S.; Sotiriou-Leventis, C. "The Effect of Compactness on the Carbothermal Conversion of Interpenetrating Metal Oxide /

Resorcinol-Formaldehyde Nanoparticle Networks to Porous Metals and Carbides," *J. Mater. Chem.* **2010**, *20*, 7456-7471.

[23] Dodge, J. "Polyurethanes and Polyureas," in "Synthetic Methods in Step-Growth Polymers;" Rogers, M. E.; Long, T. E. Eds.; Wiley: New York, **2003**, p 197.

[24] De Vos, R.; Biesmans, G. L. J. G. "Organic Aerogels," U.S. Patent No. 5,484,818 (issued: January 16, 1996).

[25] (a) Lee, J. K. "Polyurea Aerogels," U.S. Patent Application No. 2006/0211840, (publication date: September 21, 2006).

(b) Lee, J. K.; Gould, G. L.; Rhine, W. "Polyurea Based Aerogel for a High Performance Thermal Insulation Material," *J. Sol-Gel Sci. Technol.* **2009**, *49*, 209-220.

[26] Leventis, N.; Chidambareswarapattar, C.; Bang, A.; Sotiriou-Leventis, C. "Cocoon-in-Web-like Superhydrophobic Aerogels from Hydrophilic Polyurea and Use in Environmental Remediation," *ACS Appl. Mater. Interfaces* **2014**, *6*, 0000-0000 (in press).

[27] (a) Callies, M.; Quere, D. "On Water Repellency," *Soft Matter* **2005**, *1*, 55-61.

(b) Sas, I.; Gorga, R. E.; Joines, J. A.; Thoney, K. A. "Literature Review on Superhydrophobic Self-Cleaning Surfaces Produced by Electrospinning," *J. Polym. Sci. Part B: Polym. Physics* **2012**, *50*, 824–845.

(c) Shirtcliffe, N. J.; McHale, G.; Newton, M. I. "The Superhydrophobicity of Polymer Surfaces: Recent Developments," *J. Polym. Sci. Part B: Polym. Physics* **2011**, *49*, 1203–1217.

[28] (a) Rigacci, A.; Marechal, J. C.; Repoux, M.; Morena, M.; Achard, P. "Preparation of Polyurethane-based Aerogels and Xerogels for Thermal Superinsulation," *J. Non-Cryst. Solids* **2004**, *350*, 372-378.

(b) Biesmans, G.; Mertens, A.; Duffours, L.; Woignier, T.; Phalippou, J. "Polyurethane Based Organic Aerogels and their Transformation into Carbon Aerogels" *J. Non-Cryst. Solids*, **1998**, *225*, 64-68.

[29] (a) Tiger, R. P.; Badayeva, I. G.; Bondarenko, S. P.; Entelis, S. G. "Kinetics and Mechanism of Cyclic Trimerization of Isocyanates Using a Tertiary Amine-alkylene Oxide Catalytic System," *Vysokomol. Soyed.* **1977**, *A19*, 419-427.

(b) Beitchman, B. D. "Isocyanurate Syntheses via Triethylene Diamine-cocatalyst Combination," *I&EC Product Research and Development* **1966**, *5*, 35-41.

(c) Urlich, H.; Tucker, B.; Sayigh, A. A. R. "Base-catalyzed Reaction of Isocyanates. The Synthesis of 2,4-Dialkylallophanates," *J. Org. Chem.* **1967**, *32*, 3938-3941.

[30] Chidambareswarapattar, C.; McCarver, P. M.; Luo, H.; Lu, H.; Sotiriou-Leventis, C.; Leventis, N. "Fractal Multiscale Nanoporous Polyurethanes: Flexible to Extremely Rigid Aerogels from Multifunctional Small Molecules," *Chem. Mater.* **2013**, *25*, 3205-3224.

[31] Schauerte, K.; Dahm, M.; Diller, W.; Uhlig, K. "Raw Materials" in *Polyurethane Handbook*, Oertel, G. Ed., Hanser Publisher: New York, NY, 1985, pp 42-116.

[32] Sroog, C. E. "Polyimides," *Prog. Polym. Sci.* **1991**, *16*, 561-694.

[33] Meador, M. A. B.; Johnston, J. C.; Cavano, P. J. "Elucidation of the Cross-Linking Structure of Nadic-End-Capped Polyimides Using NMR of ^{13}C-Labeled Polymers," *Macromolecules* **1997**, *30*, 515-519.

[34] Meador, M. A. "Recent Advances in the Development of Processable High-Temperature Polymers," *Annu. Rev. Mater. Sci.* **1998**, *28*, 599-630.

[35] (a) Rhine, W.; Wang, J.; Begag, R. "Polyimide Aerogels, Carbon Aerogels, and Metal Carbide Aerogels and Methods of Making Same," U.S. Patent No. 7,074,880 (2006).

(b) Meador, M. A. B.; Malow, E. J.; He, Z. J.; McCorkle, L.; Guob, H.; Nguyen, B. N. "Synthesis and Properties of Nanoporous Polyimide Aerogels Having a Covalently Bonded Network Structure," *Polymer Preprints* **2010**, *51*, 265-266.

(c) Guo, H.; Meador, M. A. B.; McCorkle, L.; Quade, D. J.; Guo, J.; Hamilton, B.; Cakmak, M.; Sprowl, G. "Polyimide Aerogels Cross-Linked through Amine Functionalized Polyoligomeric Silsesquioxane," *ACS Appl. Mater. Interface* **2011**, *3*, 546-552.

[36] (a) Meyers, R. A. "The Polymerization of Pyromellitic Dianhydride with Diphenylmethane Diisocyanate," *J. Polym. Sci. A-1* **1969**, *7*, 2757-2762.

(b) Barikani, M.; Mehdipour-Atei, S. "Preparation and Properties of Polyimides and Polyamide-Imides from Diisocyanates," *J. Polym. Sci.: Part A: Polym. Chem.* **1999**, *37*, 2245-2250.

(c) Yeganeh, H.; Mehdipour-Atei, S. "Preparation and Properties of Novel Processable Polyimides Derived from a New Diisocyanate," *J. Polym. Sci.: Part A: Polym. Chem.* **2000**, *38*, 1528-1532.

[37] (a) Leventis, N.; Sotiriou-Leventis, C.; Mohite, D. P.; Larimore, Z. J.; Mang, J. T.; Churu, G.; Lu, H. "Polyimide Aerogels by Ring Opening Metathesis Polymerization (ROMP)," *Chem. Mater.* **2011**, *23*, 2250-2261.

(b) Mohite, D.; Larimore, Z.; Churu, G.; Lu, H.; Sotiriou-Leventis, C.; Leventis, N. "Polyimide Aerogels by Ring Opening Metathesis Polymerization (ROMP)," *Polymer Preprints* **2011**, *52*, 263-264.

[38] Lee, J. K.; Gould, G. L. "Polydicyclopentadiene Based Aerogel: A New Insulation Material," *J. Sol-gel Sci. Tech.* **2007**, *44*, 29-40.

[39] (a) Dawedeit, C.; Kim, S. H.; Braun, T.; Worsley, M. A.; Letts, S. A.; Wu, K. J.; Walton, C. C.; Chernov, A. A.; Satcher, J. H.; Hamza, A. V.; Biener, J. "Tuning the Rheological Properties of Sols for Low-Density Aerogel Coating Applications," *Soft Matter* **2012**, *8*, 3518-3521.

(b) Long, T. R.; Gupta, A.; Miller II, A. L.; Rethwisch, D. G.; Bowden, N. B. "Selective Flux of Organic Liquids and Solids using Nanoporous Membranes of Polydicyclopentadiene," *J. Mater. Chem.* **2011**, *21*, 14265-14276.

(c) Kovacic, S.; Jerabek, K.; Krajnc, P.; Slugovc, C. "Ring Opening Metathesis Polymerization of Emulsion Template Dicyclopentadiene Giving Open Porous Materials with Excellent Mechanical Properties," *Polym. Chem.* **2012**, *3*, 325-328.

(d) Kim, S. H.; Worsley, M. A.; Valdz, C. A.; Shin, S. J.; Dawadeit, C.; Braun, T.; Bauman, T. F.; Letts, S. A.; Kucheyev, S. O.; Wu, K. J. J.; Biener, J.; Satcher, J. H.; Hamza, A. V. "Exploration of the Versatility of Ring Opening Metathesis Polymerization: An Approach for Gaining Access to Low Density Polymeric Aerogels," *RSC Adv.* **2012**, *2*, 8672-8680.

[40] Grubbs, R. "Olefin Metathesis Catalysts for the Synthesis of Molecules and Materials," http://www.nobelprize.org/nobel_prizes/chemistry/laureates/2005/grubbs-slides.pdf (10-21-2012).

[41] (a) Blagbrough, I. S.; Mackenzie, N. E.; Ortiz, C.; Scott, A. I. "The Condensation Reaction Between Isocyanates and Carboxylic Acids. A Practical Synthesis of Substituted Amides and Anilides," *Tetrahedron Lett.* **1986**, *27*, 1251–1254.

(b) Sorensen, W. R. "Reaction of an Isocyanate and a Carboxylic Acid in Dimethyl Sulfoxide," *J. Org. Chem.* **1959**, *24*, 978–980.

Processing and Mechanical Characterization of Polyurea Aerogels

Professor Lokeswarappa R. Dharani

Department of Mechanical and Aerospace Engineering, MS&T

The polymer aerogels were created by reacting triisocyanate Desmodur N3300a and water using triethylamine as a catalyst in a solution of acetone. The aerogels created using this reaction consist of polyurea and are referred to as polyurea aerogels (PUA). Though chemically identical, three examples of PUA have been created with varying densities. The three densities investigated were 0.12 g/cm^3, 0.17 g/cm^3, 0.33 g/cm^3. These are the upper ends of the densities that are easily produced. The 0.12 g/cm^3 and 0.17 g/cm^3 recipes form a gel in one hour and then are aged in the molds for 24 hours. The amount of catalyst dictates the time it takes for a solid gel to form, the amount of catalyst in the 0.33 g/cm^3 recipe has been decreased to increase the time to produce a gel.

Testing was conducted with the knowledge that mechanical strength for tension, compression, and shear needed to be quantified. Finding the tensile and compressive properties was simple, finding the shear properties proved rather difficult. A three-point bend tests are common, samples are subjected to tension, compression, and shear forces. Extracting data for these properties is difficult for PUA due to its ductility and bi-modular behavior. Due to this, a new test was developed to determine the shear characteristics. The results from tensile, compressive and shear tests are summarized in Table 1.

The second phase of mechanical characterization consisted of dynamic tension and bending testing using dynamic mechanical analysis (DMA) and numerical simulation to develop a better understanding of structure-property response. In most cases, the mechanical properties were minimally affected when tested over a range of frequencies. In tension the previously observed increase of stiffness with density was not present. In this case the 0.17 g/cm^3 has the lowest storage modulus. Micro-scale effects such as particle stiffness, bond strength, and particle frictional coefficients were incorporated into the macro-scale structure-property relationship for the prediction of the Young's modulus. Compression simulations were performed and compared to the corresponding experiment.

Simulations were completed to determine the micro-properties such as bond strength and particle stiffness that cannot be calculated experimentally. These parameters were then used to calculate the Young's modulus of another aerogel with a similar microstructure. This would allow an estimate of the Young's modulus without laboratory testing. The diffusion limited cluster-cluster aggregation (DLCA) algorithm provided a method for creating polyurea aerogels for simulation. Particle Flow Code 3D (PFC3D) was used to simulate the particle interaction as the micro-parameters were varied.

Dynamic mechanical analysis (DMA) showed how the storage modulus (E') changes over a range of frequencies. The phase angle provided information on the damping behavior of the three densities. The output of the DLCA code, a table consisting of particle radius and its location in 3D space, was supplied to the PFC3D input file. The cube size was chosen based on the largest cell size possible while maintaining computational efficiency. Once the model is created in PFC3D it is calibrated by estimating initial values for the particle stiffness and bond strength then adjusting these values until the modulus in compression of the simulation matches the experimental value.

In the DMA, frequency scans of polyurea aerogel showed that frequency has a minimal effect of the storage modulus in the frequency range tested. The tension test indicated that the 0.17 g/cm^3 more efficiently damped the oscillatory motion induced by the DMA than the other two

densities. Testing has concluded that polyurea aerogels are mechanically strong and insensitive to mid-range frequencies. PUA could prove to be a useful new material in a wide variety of engineering structures if processes could be developed to keep production costs to a minimum.

Table 1. Compiled Results from Testing

Tension	PUA Density	Young's Modulus (MPa)	Yield Stress (MPa)	Failure Stress (MPa)	Failure Strain (%)
	0.12 g/cm^3	24.1 ±0.5	0.7 ±0.03	1.1 ±0.08	12.5 ±2.3
	0.17 g/cm^3	37.2 ±1.3	1.0 ±0.2	1.7 ±0.1	13.5 ± 3.0
	0.33 g/cm^3	102 ±7.2	2.93 ±0.4	3.9 ±0.2	6.0 ± 0.6
Compression	PUA Density	Young's Modulus (MPa)	Yield Stress (MPa)		
	0.12 g/cm^3	11.7 ±4.4	0.4 ±0.01		
	0.17 g/cm^3	19.3 ±4.2	0.7 ±0.1		
	0.31 g/cm^3	69.0 ±17.9	2.4 ±0.3		
3 Point Bend	PUA Density	Young's Modulus (MPa)	Yield Stress (MPa)		
	0.12 g/cm^3	33.1 ±2.5	1.03 ±0.1		
	0.17 g/cm^3	62.7 ±6.4	1.9 ±0.1		
	0.31 g/cm^3	137.9 ±13.1	4.65 ±0.4		
Shear	PUA Density	Shear Modulus (MPa)	Yield Stress (MPa)	Failure Stress (MPa)	
	0.12 g/cm^3	8.3 ±0.6	0.2 ±0.02	0.4 ±0.03	
	0.17 g/cm^3	11.7 ±0.7	0.4 ±0.04	0.7 ±0.08	
	0.31 g/cm^3	37.9 ±2.5	1.2 ±0.2	1.6 ±0.3	

Conclusions

The results for bending are for informational purposes only and should not be use for preliminary design calculations for strength or stiffness, although the information provided by the tension, compression, and shear tests can be used to calculate strength and stiffness in bending. The information in Table 1 can be used for preliminary design calculations of structures experiencing static loads. Structures subjected to dynamic loads or extreme environments would require additional testing. Fatigue and creep testing would need to be completed to determine the behavior of PUA under long-term conditions. Dynamic mechanical analysis can be used to determine strength and stiffness under varying strain rates and temperatures.

PUA has proven to be mechanically strong, especially in terms of strength to weight. PUA can take extreme loads under compression; in the case of 0.31 g/cm^3 was able to support forty thousand times its own weight before yielding and over three million times its weight at the highest strain values. From the available information PUA would be well suited to an application where low weigh, high stress, and high strain were necessary as long as loading only occurred once. Such applications could include impact-absorbing structures used in automobiles. If the manufacturing costs can be kept low, PUA could have a number of engineering applications.

The results indicate that polyurea aerogels are not particularly sensitive to various mid-range frequencies. The change in storage modulus across the tested range was minimal. The 0.17 g/cm^3 damped the oscillatory motion more effectively in tension than the other two densities. Compression simulations using PFC3D were completed using the PUA model. Simulations showed that the shear and normal stiffness of the particles were equivalent rather than a ratio as suggested by literature.

Cost-Effective Synthesis of Vanadia Aerogels and Derivatives for Applications in Thermochromics, Energy Storage and Ballistics

Professor Jeffrey Winiarz

Department of Chemistry, MS&T

We have successfully fabricated vanadium oxide (VO_x) aerogels using $VOCl_3$ instead of $VO(OPr)_3$. The primary motivation for this substitution resides in the relative cost. As such, we have reduced the cost associated with the synthesis of VO_x aerogels by a factor of ~10. Gels produced with this precursor have a nanoworm micromorphology identical to those fabricated using the alkoxide method, as seen in **Figure 1**. Initial characterizations demonstrate that the wet gels are also much sturdier than alkoxide wet gels leading to improved processability. The native gels have a density of 103 mg/mL and are macroporous. Characteristic of aerogel materials, they also exhibit an extremely large BET surface area of 102 m^2/g. The durability of the vanadium oxide aerogels can in part be attributed to the fact that shrinkage is negligible during aging and supercritical drying. The gels can be crosslinked using Desmodur N-3200 bifunctional isocyanate to produce mechanically strong X-aerogels (**Figure 2**). These gels can be used to form VN aerogels using aromatic isocyanate crosslinking and pyrolysis under NH_3. We have also modified this method to produce high-quality VO_2 films (**Figure 3**), which have potential application as a thermochromic coating for energy efficient windows. A provisional patent application for this method has been filed through the Missouri S&T Technology Transfer office.

Additionally, vanadium oxide aerogels have been fabricated using V_2O_5 as a vanadium source, potentially lowering cost further. These gels were found to have particulate morphology and are also susceptible to isocyanate crosslinking.

We have developed a facile hydrothermal method for synthesizing uniform $Li_\alpha V_6 O_{13}$ (**Figure 4**) and $VO_2(B)$ nanoparticles which have application as Li-ion battery cathode materials.

Current work on vanadia aerogels involves elucidation of the gelation mechanism via ^1H, ^{13}C, and ^{51}V NMR. We are investigating the crystalline structural of the $Li_\alpha V_6 O_{13}$ nanoparticles using the high-resolution x-ray and neutron diffraction facilities at Argonne National Laboratory and Oak Ridge National Laboratory, respectively. We are also developing alternative electrolyte solvents appropriate for *in-operando* neutron diffraction of Li-ion battery electrodes.

Future work involves the characterization of the thermochromic properties of VO_2 films, electrochemical properties of $Li_\alpha VO_x$ nanoparticles, and optimization of vanadia gel fabrication.
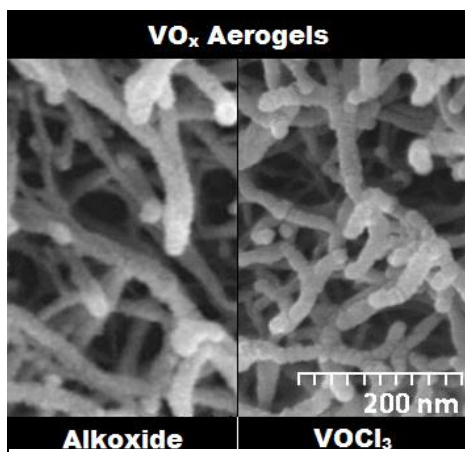
Figure 1. SEM image of native vanadia aerogels.

Figure 2. Photo of vanadia gels.
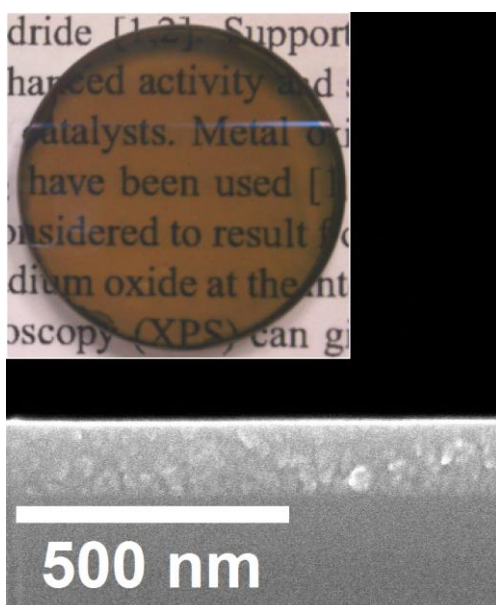
Figure 3. SEM image of VO_2 film cross-section with inset photo on a 1" diameter silica substrate.
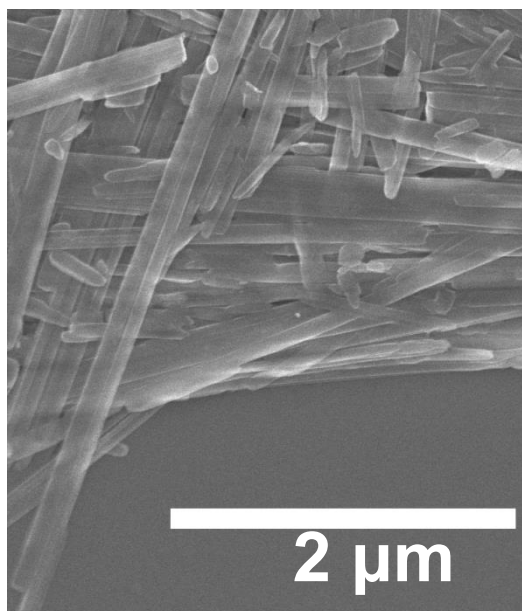
Figure 4. SEM image of $Li_\alpha V_6 O_{13}$ nanoparticles.

Flame Synthesis of VOx and ZnO Nanoparticles

Professor Yangchuan Xing

Department of Chemical Engineering, MS&T

1. Flame synthesis of vanadia (VOx) nanoparticles and their conversion to nanoporous VC

A counterflow diffusion flame (CDF) reactor was used to synthesize Vanadium oxide nanoparticles. It consists of two vertical channels of rectangular cross sections that are positioned opposite to each other. The flame established using the combustion gases produces a temperature gradient between the mouth of the burner and the flame. Particle morphology can be easily controlled using the CDF reactor because of the different chemical environment present on either sides of the flame. The important point that needs to be considered is that the flame should be nearly flat for producing nanoparticles of uniform size and shape. This flat flame can be obtained by using a honeycomb mesh on the rectangular cross sections. The schematic depicting the setup for a CDF reactor is shown in Fig. 1.
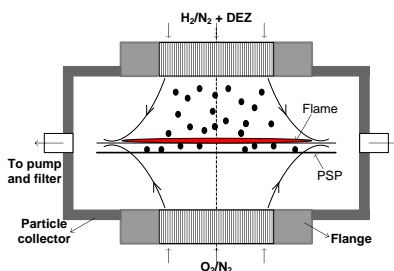
Fig. 1 Schematic showing of the CDF reactor for making metal oxide nanoparticles.
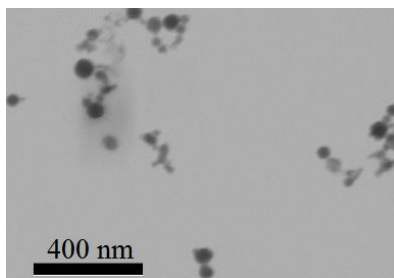
Fig. 2 TEM image of the VOx nanoparticles from the CDF reactor.
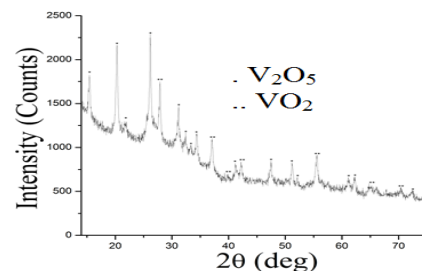
Fig. 3 XRD shows phases of the VOx nanoparticles from the CDF reactor.

The precursor used for the production of vanadium oxide nanoparticles was vanadium oxytripropoxide. The precursor was filled in a gas tight syringe and introduced using a syringe pump. The flow rate for the production of vanadium oxide nanoparticles was 2 ml/hr. It has be to noted that vapor pressure of vanadium oxytripropoxide ar room temperature is very low and hence, it has to be heated to around 70-75°C, where it has a vapor pressure of 20 Pa. Heating tape is wound across the line that carries the precursor and the gas line, and the heating tape was then connected to an auto transformer to control the rate of heating.

Fig. 2 shows the STEM image of the vanadium oxide nanoparticles. It can be clearly seen that the particles are spherical in shape with an average size of approximately 50 nm. The morphology of the particles is spherical since they are produced in a flame and hence the smaller particles tend to get sintered to form a larger particle. The vanadium oxide particles produced were then used to synthesize vanadium carbide. The vanadium oxide powder obtained from the CDF was then analyzed using X-ray diffraction (XRD) and scanning electron microscope (SEM) in the STEM mode. Fig. 3 shows the XRD pattern of the VOx particles with two main phases of V_2O_5 and VO_2.

These nanoparticles were used as precursors to make nanoporous VC material. The metal oxides were weighed and added to appropriate proportions of tartaric acid and distilled water. The mixture was refluxed for 24 hrs. After the refluxing process is over, the mixture is then put on a hot plate for 15-20 mins at approximately 100°C to remove water. The resultant powder was then pyrolyzed at 1500°C for 24 hrs in a tubular furnace.

XRD analysis was done on the resultant products and the corresponding image is shown in Fig. 4. It shows the formation of VC and V_8C_7 as the products from pyrolysis. Hence, VC was successfully synthesized by using flame made vanadium oxide as the precursor. Images from the SEM analysis of the VC powder obtained from pyrolysis are shown in Fig. 5. From the images it can be clearly seen that the VC powder product obtained from high temperature pyrolysis has a very large particle size (~300 nm, inset) compared to the initial vanadium oxide particle size. This might be due to the effect of sintering of the powder during the pyrolysis process. Our aim is to synthesize VC powder using vanadium oxide powder as the precursor without any large change in the shape of the particles. This has been under further study.
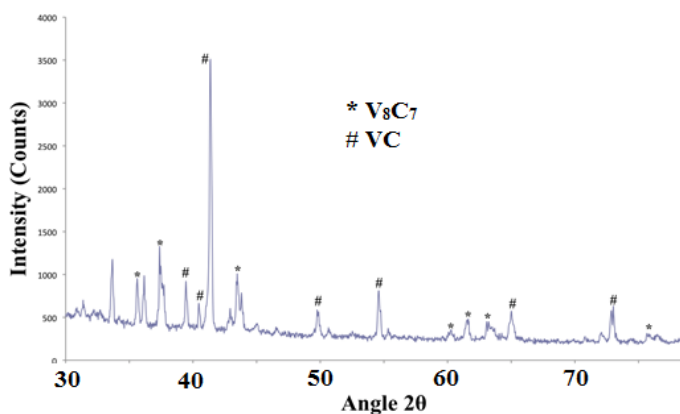
Fig. 4 XRD pattern of the pyrolysis product obtained from refluxing tartaric acid and distilled water
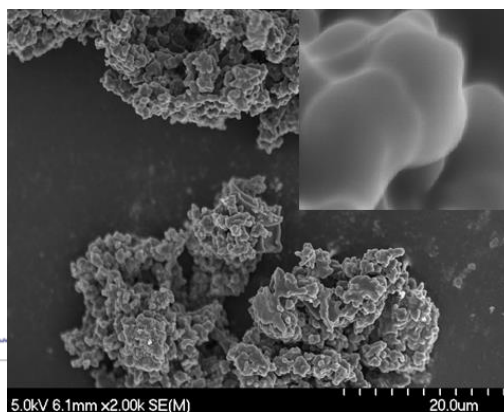
Fig. 5 SEM images of the porous VC nanoporous material. The inset shows a high magnification image.

2. Flame synthesis of ZnO nanoparticles

This work has been to make ZnO nanoparticles in the CDF reactor. ZnO nanoparticles showed a nanorod morphology (see Fig. 6). ZnO can be made into many nanostructures that have unique properties for advanced applications, such as piezoelectric and pyroelectric materials. ZnO nanorod is one of the nanostructures that possess advanced properties. We show the flame process can be used to continuously synthesize aerosols of ZnO nanorods in large quantities. Unlike previous work, our process shows that pure ZnO nanorods can be made in a freestanding form rather than growing on a substrate surface. It was found that the ZnO nanorods preferentially grow in the thermodynamically stable direction [001] in the gas phase with different aspect ratios, depending on flame process conditions. The ZnO nanorod aerosols are highly crystalline and have a hexagonal geometry. Raman and photoluminescence spectroscopic studies showed that there are no structural defects in the nanorods, which have energy band gap of 3.27 eV in the near UV region. A journal paper has been published on this work [1].
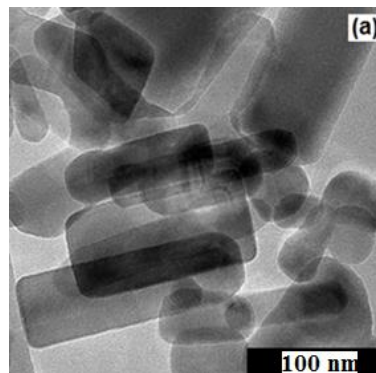
Fig. 6 TEM image of ZnO nanorods made in the CDF reactor.

3. References

[1]   Gandikota, V.; Xing, Y. "Flame Aerosol Synthesis of Freestanding ZnO Nanorods," *Advances in Nanoparticles* **2014**, *3*, 5-13.

Development and Self-Assembly of Multifunctional Inorganic-Polymer Hybrid Materials for Solar Energy Applications

Professor Zhonghua Peng

Department of Chemistry, University of Missouri- Kansas City

1.   Major Research Accomplishments

The primary objectives of the original proposal are to develop various inorganic-polymer hybrid materials, study their self-assembly processes using innovative characterization techniques, and explore their potential applications as new multifunctional materials. During the three years under this grant support, we have made significant progress in a number of research fronts [1-20], which are summarized in the following sections.

1.1   Mechanochemical approach to composition-tunable semiconducting nanoparticles

We have demonstrated that a simple high energy ball milling technique can be used to
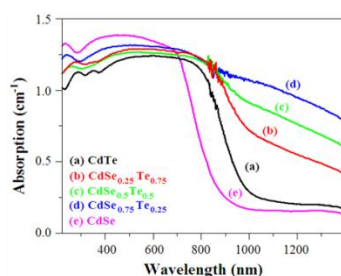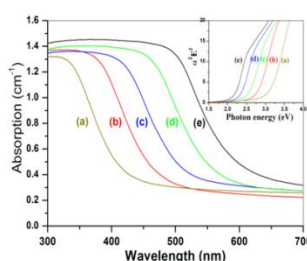
prepare uncapped semiconducting nanocrystals in large scale and with convenient composition tuning. Ternary $CdSe_{1-x}S_x$ [1], $CdTe_{1-x}Se_x$ [2], and $Zn_{1-x}Cd_xS$ nanocrystals as well as carbon nanodots [3] and C-doped TiO_2 nanocrystals have been successfully prepared. The resulting nanocrystals have average sizes smaller than 9 nm (2-20 nm range with majority around 5 nm) and are chemically homogenous. Ternary CdTeSe nanocrystals are found to exhibit strong near IR (up to 1400 nm) absorption [2].

1.2   Self-assembly of charged nanoparticles

We have discovered that surface-charged nanoparticles ($CdSe_{1-x}S_x/Na_2S$ in aqueous or methanol solution [1], carboxylic acid-functionalized C-dots in water [3], and carboxylate-functionalized C-doped TiO_2 in water) self-assemble into uniformly sized single-shell hollow vesicles. Such vesicles are being explored for biomedical and energy-related applications.
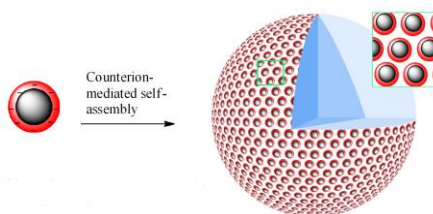
1.3   C-dots for solar cell applications

We have demonstrated for the first time that the aqueous soluble carbon nanoparticles (CNPs) can be utilized as an interfacial layer between TiO_2-coated ZnO nanorod arrays and P3HT
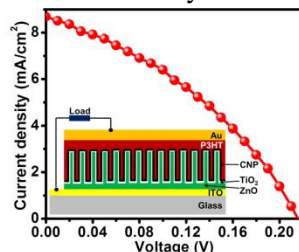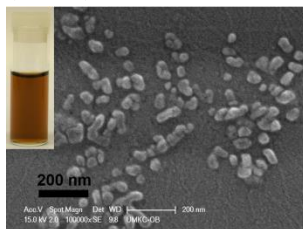

polymer, forming close and intimate contacts with both TiO_2 through carboxylic acid binding and P3HT polymer presumably by way of π–π interaction [3]. As a result, the infiltration of P3HT into the space among nanorod arrays and the formation of top P3HT cover layer are both improved.

The resulting HSCs showed the highest photocurrent ever reported among ordered heterojunction HSCs based on ZnO nanorod arrays and P3HT. The V_{OC} though is far from satisfactory. Using CNPs with narrower size distribution may hold the promise of overcoming this hurdle. While that remains to be seen, the concept of using aqueous soluble CNPs as an interfacial layer to improve the device performance of HSCs is clearly validated.
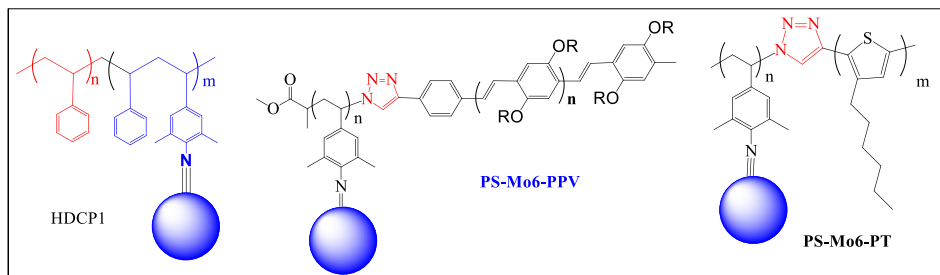
1.4 Hybrid diblock copolymers containing coordinatively binded CdSe nanoparticles

Hybrid rod-coil diblock copolymers containing coordinatively binded CdSe nanoparticles have been synthesized. Albeit their low CdSe nanoparticle loading of less than 50% and the short rod block length, simple single-layer solar cells fabricated from the hybrid copolymers showed significantly improved performance over their corresponding diblock copolymers without CdSe attachment [4].
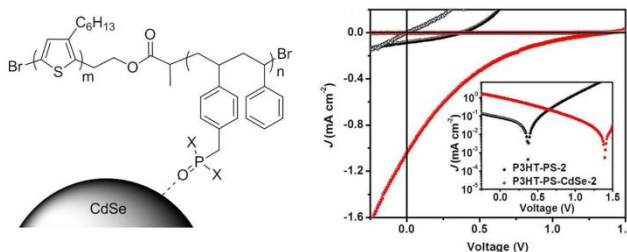
1.5 Hybrid diblock copolymers containing polyoxometalates (POMs)

A major research focus of this ARO-funded effort is directed towards the synthesis of POM-containing diblock copolymers (DCPs). Both coil-coil and rod-coil hybrid diblock copolymers have been synthesized. A rod-coil diblock copolymer with POM attached to the coil block can be considered a donor-acceptor diblock copolymer. Thus, our motivation to such hybrid rod-coil diblock copolymers is twofold: to study their complex phase behavior, identify and ultimately control the hierarchical orders, and to explore such hybrids as novel functional materials, for example photovoltaic materials. We have successfully synthesized two series of POM-containing rod-coil diblock copolymers, one based on the PPV rod block (PS-Mo6-PPV) and the other on the poly(3-hexylthiophene) rod block (PS-Mo6-PT) [5].

The structures of all hybrid DCPs have been thoroughly characterizations using ^{1}H NMR, FTIR, GPC, and MALDI-TOF measurements. Their thermal (DSC/TGA), optical (UV/Vis and FL emission), and electrochemical (CV) properties have also been carefully studied.

To study the morphology of the spin-coated or drop-cast films, a multi-functional scanning probe microscopy which generates simultaneously the topographical and the charge impedance images has been set up. A network analyzer (Rhode & Schwarz


28
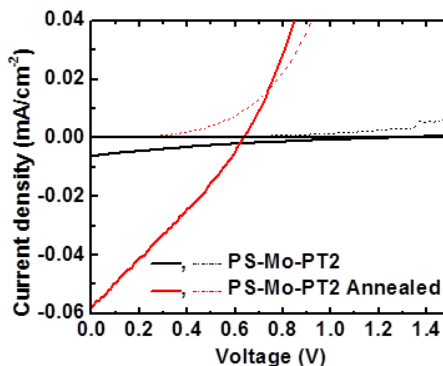
ZVB4) was purchased using the ARO support. By integrating this instrument into our currently existing atomic force microscopes, we are able to perform simultaneous surface morphology and charge impedance imaging with nanometer resolution from DC to microwave frequency range. Also integrated to the instrument is a light source (a laser is currently under consideration to be added to the system) so that photoconductive scanning probe microscopy imaging can be performed.

Current-sensing AFM studies show that the spin-coated films of the PS-PPV film show no conducting domains at all. After cluster attachment, only some minor conducting areas are noticed. These results indicate that both PS-PPV and PS-Mo6-PPV films exhibit negligible phase separation. PS-PT DCPs and PS-Mo6-PT DCPs, however, show very clear conducting domains. The film morphology is found to be sensitive to the size of the PT block and also depends on the solvent. Solar cells with the configuration of ITO/PEDOT:PSS/HDCP/Ca/Al have been fabricated [6]. A one-order of magnitude higer efficiency (0.010%) was observed from the annealed photovoltaic device in comparison to that (0.001%) of the unannealed device. While good open circuit voltage (1.25 V) is observed for the pristine film, the short circuit photocurrent is dismally low. Annealing improves the photocurrent by one order of magnitude and also the fill factor, presumably due to the formation of desired phase-separated domains. The overall photocurrent is however still very low, likely due to the poor photoinduced charge transfer from the PT backbone to the POM cluster.

1.6   Solution self-assembly of POM-polymer hybrids

The solvent dependence of film morphology prompted us to study the aggregation behavior of hybrid polymers in solutions. Our studies on a POM-containing conjugated polymer show that the hybrid polymer behaves very differently in different solvents [7]. In a non-polar solvent such as toluene, the counter ion (tetrabutyl ammonium) is closely associated with the
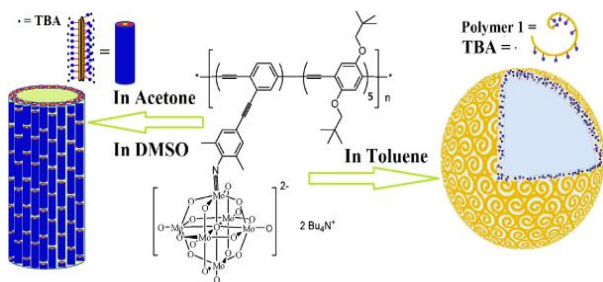
POM cluster anion. With the conjugated polymer backbone solvaphilic while the POM clusters solvaphobic, the hybrid DCP self-assembles into hollow spheres or vesicles. In a polar solvent such as acetone or DMSO, the counter ions are dissociated from the cluster anion, making the hybrid polymer polyelectrolyte-like, which self-assemble into tubes.
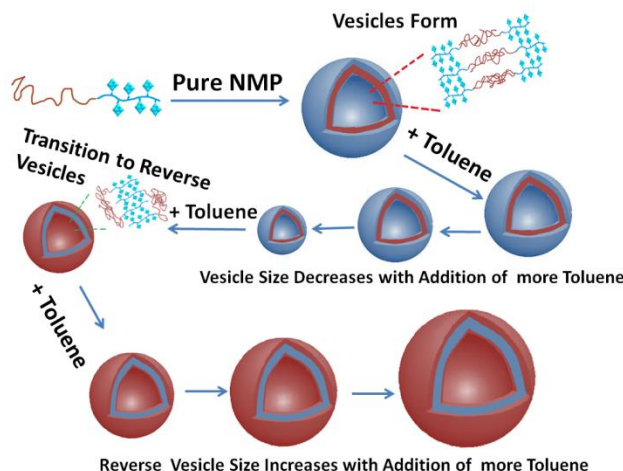

The solution self-assembly behavior of the three PS-Mo6-PT hybrid diblock copolymers has also been studied. In NMP, the three hybrid diblock copolymers tend to aggregate to form vesicles with the PS-Mo6-PT3 having the largest size. This is expected due to its significantly longer non-polar PT block length than those of PS-Mo6-PT1 and PS-Mo6-PT2. The polar coil block is exposed to the polar solvent while the non-polar PT block forms the inner layer. When toluene, a non-polar solvent, is added, the interaction between the PS-Mo6 polar head groups is weakened, since the polar

PS-Mo6 block does not like the non-polar solvent, leading to smaller vesicles. When the toluene fraction reaches a certain value, the overall solvent quality becomes non-polar, the bilayer vesicular structures switch positions with the PT block now facing the solvent while the cluster block staying inside and away from the solvent, forming reversed vesicles.

1.7   *Organically functionalized nanoparticles*

In addition to hybrids based on POM-containing and CdSe nanoparticle-containing diblock copolymers, other types of polymer hybrids have also been explored. One is core-shell nanoparticles where polymer shell grows out of a variety of nanoparticle cores through environmentally friendly enzymatic polymerization. In addition to being "greener," the enzymatic polymerization also allows the synthesis of some polymers which are otherwise inacc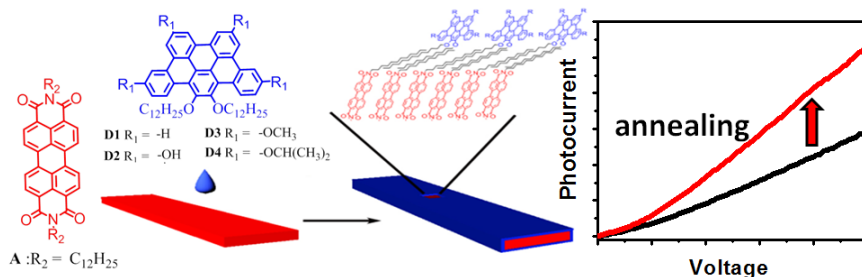essible through chemical means, e.g. poly(phenols). Gold nanoparticles (Au NPs) and silica nanoparticles have been successfully functionalized with alkyl chains bearing terminal azido groups. The azido end is available for further modification and functionalization using "click" reaction with ethynyl-functionalized small molecules, polymer chains, and POMs. We have been able to achieve *ca.*50 % "click" efficiency in the preliminary studies. The unprecedented POM functionalized NPs are interesting materials for catalysis and molecular electronics.
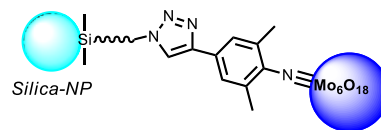
1.8   *Other unique conjugated systems*

While it has been demonstrated, in quite a few systems, that donor-acceptor diblock copolymers show better photovoltaic efficiencies than their corresponding donor/acceptor blends, all donor-acceptor diblock copolymers reported so far still show disappointing device performance. This is probably a result of low charge carrier mobility intrinsic to many organic conjugated systems. While having closely packed POMs will likely make the electron transport facile, hole transport through the aggregated conjugated polymer segment may need further improvement. Thus, efforts have been devoted towards the synthesis of new conjugated systems with high charge mobilities.

1)   *New soluble polycyclic aromatic hydrocarbon molecules as electron donors:* we have synthesized a series of electron donor molecules (D1-D4) that share the same π-conjugation core, but modified with different side groups [8]. Perylenediimde fibers coated with such donor molecules showed dramatically different photocurrent response [9]. It was found that the nanofibers coated with homogeneously and molecularly distributed donor molecules (such as D4) exhibit the highest photo-current, whereas those coated with s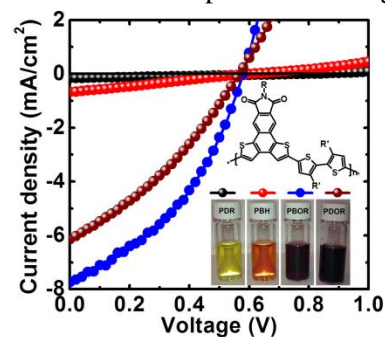egregated donor aggregates (such as D1-D3) show much lower photocurrent under the same illumination conditions. The aggr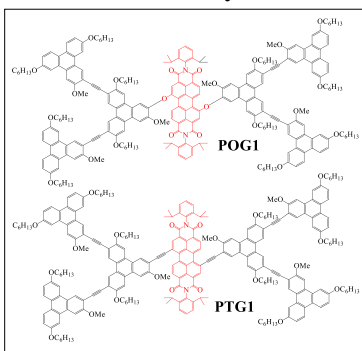egation of donor molecules on the surface of the fibers may lead to the buildup of local electrical field which hinders the charge separation of the photogenerated electron-hole pairs. The different morphologies of molecular aggregates were mostly the result of side group modification of the donor molecules. Such structural effect was more clearly manifested by investigating the structure and morphology change of the drop-cast films upon solvent vapor annealing.

2) *New donor-acceptor conjugated polymers.* Four donor-acceptor alternating conjugated copolymers based on a new imide-functionalized naphtho[1,2-b:3,4-d′]dithiophene monomer and 2,2'-bithiophene comonomers have been synthesized and characterized [10]. Varying the substituents at the 3,3' positions of the comonomer unit has a profound effect on the conformational twist of the backbone, and consequently the optical, redox and photovoltaic properties of the copolymers. Bulk heterojunction solar cells of these copolymers blended with [6,6]-phenyl-C71-butyric acid methyl ester show power conversion efficiencies up to 2.45%.
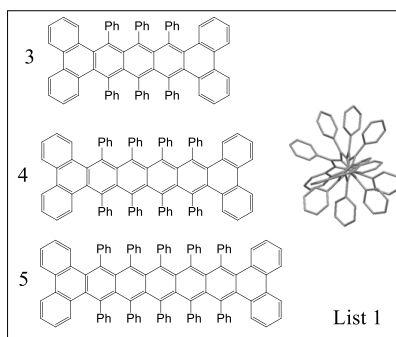
3) *Dendritic donor-acceptor systems.* We have previously shown that triphenylene-based conjugated unsymmetrical dendrons (TPA dendrons) are promising light-harvesting systems [11]. To confirm that they are also excellent electron donors in a photoinduced electron transfer system, the TPA dendrons were covalently linked to the bay positions of a perylenebisimide (PBI) core [12,13]. While both the TPA donor G1 and the PBI core (POB) are highly fluorescent separately, the covalently jointed system (POG1 & PTG1) exhibit very weak fluorescence. In other words, both the donor emission and the acceptor emission are nearly completely quenched. The fluorescence quenching is thought to be due to the photoinduced electron transfer from the TPA donor to the PBI acceptor, which is confirmed by their frontier orbital levels obtained by cyclic voltammetry.

4) *Highly twisted polycyclic aromatic hydrocarbons*: One interesting organic system is the highly twisted polycyclic aromatic hydrocarbons (PAHs). While PAH and acenes have been studied extensively for their optical properties, we have developed a synthetic procedure to synthesize a series of acene that are highly twisted (some are chiral and helical) and linear ribbons. Using this approach, we are able to systematically investigate the effect of the twist, end units, substituents, and length of the ribbon on their corresponding spectral properties. The overall study will help to further understand these effects, which would result in improved optoelectronic material. To date, approximately 10 acenes have been characterized with end-to-end twists greater than 60°. Of those 10, only two possess an end-to-end twist greater than 100° (one shown as 3 in list 1). We have successfully synthesized hexacene derivative 4. X-ray analysis indicates that 4 possesses the largest twist ever reported of 176.5°. We are currently synthesizing the corresponding heptacene 5 and the derivatives of 4 and 5 with different capping groups.

5) *High hole mobility of solution processed thin films of a polycyclic thiophene-based small molecules.* We synthesized a new soluble thiophene-containing polycyclic compound and discovered that spin-coated thin films of this compound exhibit high space-charge limited current (SCLC) hole mobility up to 8.72×10^{-2} cm^2 V^{-1} s^{-1} [14]. This value is amongst

the highest reported hole mobilities obtained by either filed-effect transistor or SCLC method for solution-processed small-molecule organic semiconductors.
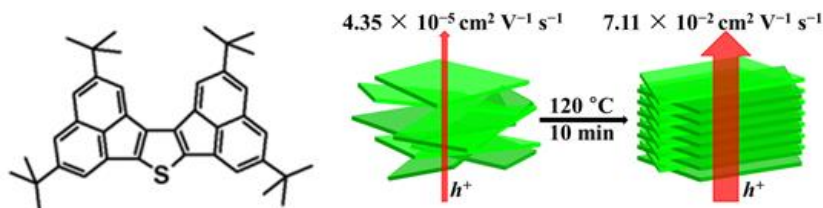
1.9   Free volumes and multi-layer structures in nano-scale films and nanocomposites studied by positron annihilation spectroscopy (PAS)

(1).   *Upgrading slow positron beam at UMKC.* With the ARO support, we are able to upgrade our existing slow positron beam including the new two dimensional (2D) extension system and data acquisition system electronics for the variable mono-energy slow positron beam at UMKC. The improvements include 1) Using 2D coincident technique to obtain a much better energy resolution with improved 2 orders of magnitude in background reduction, 2) Extending the beam to a location with better sample manipulation, and 3) Installing a new 2D-data acquisition system which will be able to collect data in a better efficiency.

(2) *Free volumes in ZnO-polyurethane nanocomposites.* The free-volume properties in a system of zinc oxide (ZnO) nanoparticles (20 nm) dispersed in waterborne polyurethane (WBPU) were measured using positron annihilation lifetime spectroscopy [15]. Two glass-transition temperatures (Tg), lower Tg ~ 220 K and higher Tg ~ 380 K of the ZnO/WBPU nanocomposites, were found and both increase with increasing zinc oxide content from 0 % to 5 %. These two glass transitions are interpreted from two segmental domains of WBPU; the lower Tg is due to soft aliphatic chains and high Tg is due to polar hard microdomains, respectively. The increase in Tg with the addition of ZnO fillers is mainly attributed to interfacial interactions through hydrogen bonding, van der Walls forces, and electrostatic forces between the polymer matrix and zinc oxide nanoparticles. These results are supported by the data from the dynamic mechanical thermal analysis (DMTA). The relationship between the free volume obtained from nanoscopic positron method and the physical crosslink density from macroscopic DMTA method as a result of microphase separation of hard and soft segments in polyurethane is found to follow an exponential function. Chemical properties and surface morphology of nano-composites were examined by Fourier transform infrared spectroscopy (FTIR) and by atomic force microscopy (AFM).

(3) *Glass transition in SWCNT/PS nanocomposites.* Positron annihilation spectroscopy was employed to study the free volume properties at three levels of interfacial interaction between Polystyrene and carbon nanoparticles, polystyrene grafted oxidized single wall carbon nanotubes (SWCNT) composites (PS/g-SWCNT-COOH), Polystyrene oxidized Single wall carbon nanotubes (PS/SWCNT-COOH) and polystyrene carbon nanofiber composites (PS/CNF) which represent covalent bonding, hydrogen bonding and Van der Waal's interaction [16-18]. Results of temperature dependence of orthopositronium lifetimes for the three composites show that covalent PS/g-SWCNT-COOH has the highest Tg with changing concentration of SWCNT-COOH in PS matrix in comparison with PS/SWCNT-COOH and PS/CNF, which indicates a correlation between the strength of interfacial interaction and the glass transition temperature. The results are supported by the results from DSC and FTIR data. This is in collaboration with Prof. W. Ford of Oklahoma State University.

2.   References

[1]   Tan, G.; Li, S.; Murowchick, J. B.; Wisner, C.; Leventis, N.; Peng, Z. "Preparation of Uncapped CdSe$_{1-x}$S$_x$ Semiconducting Nanocrystals by Mechanical Alloying," *J. Appl. Phys.* **2011**, *110*, 124306.

[2]   Li, S.; Tan, G.; Murowchick, J. B.; Wisner, C.; Leventis, N.; Xia, T.; Chen, X.**;** Peng, Z. "Preparation of Uncapped CdSexTe1-x Nanocrystals with Strong Near-IR Tunable Absorption," *J. Electronic Mater.* **2013**, *42(12)*, 3373-3378.

[3]   Li, Y.; Li, S.; Jin, L.; Murowchick, J. B.; Peng, Z. "Carbon Nanoparticles as an Interfacial Layer Between TiO$_2$-coated ZnO Nanorod Arrays and Conjugated Polymers for High-Photocurrent Hybrid Solar Cells," *RSC Adv.* **2013,** *3(37)*, 16308 − 16312.

[4]   Li, S.; Li, Y.; Wisner, C. A.; Leventis, N.; Peng, Z. "Synthesis, Optical Properties and Photovoltaic Applications of Hybrid Rod−Coil Diblock Copolymers with Coordinatively Attached CdSe Nanocrystals," submitted to *RSC Adv.*, **2014**.

[5]   Chakraborty, S.; Jin, L.; Li, Y.; Liu, Y.; Dutta, T.; Zhu, D.-M.; Yan, X. Z**.**; Keightley, A.; Peng, Z. "Synthesis, Characterization, and Photovoltaic Applications of Polyoxometalate-Containing Rod-Coil Diblock Copolymers," *Eur. J. Inorg. Chem.* **2013**, 1799-1807.

[6]   Li, Y.; Jin, L.; Charaborty, S.; Li, S.; Lu, P.; Zhu, D.; Yan, X.; Peng, Z. "Femtosecond Time-Resolved Fluorescence Study and Photovoltaic Properties of Polyoxometalate-Containing Rod-Coil Diblock Copolymers," *J. Polym. Sci. B* **2014**, *52(2)*, 122-155.

[7]   Yin, P.; Jin, L.; Li, D.; Cheng, P.; Vezenov, D. V.; Bitterlich, E.; Wu, X.; Peng, Z.; Liu, T. "Supramolecular Structures of Conjugated Polymers with Polyoxometalate-Containing Side Chains in Polar and Nonpolar Solvents," *Chem. Eur. J.* **2012**, *18*, 6754-6758.

[8]   Chou, C.; Li, Y.; Che, Y.; Zang, L.; Peng, Z. "Synthesis, Self-assembly and Photovoltaic Applications of Tribenzopentaphene Derivatives," *RSC Adv.* **2013**, *3(43)*, 20666 - 20672.

[9]   Huang, H.; Chou, C.; Che, Y.; Li, L.; Wang, C., Yang, X.; Peng, Z.; Zang, L. "Morphology Control of Nanofibril Donor-Acceptor Heterojunction to Achieve High Photoconductivity: Exploration of New Molecular Design Rules," *J. Am. Chem. Soc.* **2013**, *135(44)*, 16490-16496.

[10]   Dutta, T.; Li, Y.; Thornton, A. L.; Zhu, D.; Peng, Z. "Imide-Functionalized Naphthodithiophene Based Donor-Acceptor Conjugated Polymers for Solar Cells," *J. Polym. Sci. A* **2013**, *51*, 3818-3828.

[11]   Dutta, T.; Che, Y.; Zhong, H.; Laity, J. H.; Dusevich, V.; Murowchick, J. M.; Zang, L.; Peng, Z. "Synthesis and Self-assembly of Triphenylene-Containing Conjugated Macrocycles," *RSC Advances* **2013**, *3*, 6008-6015.

[12]   Bagui, M.; Dutta, T.; Chakraborty, S.; Melinger, J. S.; Zhong, H.; Keightley, A.; Peng, Z. "Synthesis and Optical Properties of Triphenylene-Based Dendritic Donor Perylene Diimide Acceptor Systems," *J. Phys. Chem. A* **2011**, *115(9)*, 1579–1592.

[13] Bagui, M; Dutta, T.; Zhong, H.; Li, S.; Chakraborty, S.; Keightley, A.; Peng, Z. "Synthesis and Optical Properties of Perylene Diimide Derivatives with Triphenylene-Based Dendrons Linked at the Bay Positions through a Conjugated Ethynyl Linkage," *Tetrahedron* **2012**, *68*, 2806-2818. doi:10.1016/j.tet.2012.02.008.

[14] Li, Y.; Clevenger, R. G.; Jin, L.; Kilway, K. V.; Peng, Z. "High SCLC Hole Mobility in Solution-Processed Thin Films of a Polycyclic Thiophene-Based Small-Molecule Semiconductor," in preparation, **2014**.

[15] Awad, S.; Chen, H.; Chen, G.; Gu, S.; Lee, J. L.; Abdel-Hady, E. E.; Jean, Y. C. "Free Volumes, Glass Transitions, and Cross-links in Zinc Oxide /Waterborne Polyurethane Nanocomposites," *Macromolecules* **2011**, *44*, 29-38.

[16] Liao, K.-S. Chen, H.; Awad, S.; Yuan, J.-P.; Hung, W.-S.; Lee, K.-R.; Lai, J.-T.; Hu, C.-C.; Jean, Y.C. "Determination of Free-volume Properties in Polymers Without Orthopositronium Components in Positron Annihilation Lifetime Spectroscopy," *Macromolecules* **2011**, *44*, 6818-6826.

[17] Award, S.; Chen, H.M.; Grady, B. P.; Paul, A.; Ford, W. T.; Lee, L. J.; Jean, Y.C. "Positron Annihilation Spectroscopy of Polystyrene Filled with Carbon Nanomaterials," *Macromolecules* **2012**, *45*, 933-940.

[18] Chen, H.; Van Horn, J. D.; Jean, Y.C. "Applications of Positron Annihilation Spectroscopy to Life Science,*" Defect and Diffusion Foru*m **2012**, *331*, 275-293.

[19] Li, Y.; Lu, P. F.; Yan, X. Z.; Jin, L.; Peng, Z. "Non-Aggregated Hyperbranched Phthalocyanines: Single Molecular Nanostructures for Afficient Semi-opaque Photovoltaics," *RSC Advances* **2013**, *3(2)*, 545-558.

[20] Kuroda, D. G.; Singh,C. P.; Peng, Z.; Kleiman, V. D. "Exploring the role of phase modulation on photoluminescence yield," *Faraday Discuss.* **2011**, *153*, 61-72.

Development and Study of Amine Sensors Based on Metal Nanoparticle-Doped Polyaniline

Professor Frank D. Blum

Department of Chemistry, Oklahoma State University

Our group has demonstrated how a new synthesis technique, developed in our labs can be used to make gas sensors that are significantly more sensitive than those made in more conventional ways. We have developed a photo-assisted technique producing, in a single step, PANI nanofibers on planar substrates [1]. This simple technique uses aniline, water, an acid dopant, an oxidant such as ammonium persulfate, and a metal ion. Initially, we discovered that the materials without the metal could be made into polyaniline nanofibers using gamma-radiation from a nuclear reactor after shutdown [2]. We also discovered that with the addition of certain metal ions to the solution, nanometal particles, embedded in conducting polymer nanofibers resulted [3]. These materials could be photopolymerized with UV radiation, making them suitable for lithographic applications [1].

An interdigitated array of electrodes made from PANI nanofibers is shown in Figure 1 [4]. This type of array was used as the sensor for vapors. A drop of precursor solution was placed on it, followed by irradiation with UV light. A micrograph of the resulting material on the surface is shown in Figure 2. The conducting nanofibers (or mesh) of polyaniline are apparent in the figure [5].

Fig. 1. Arrays used for PANI sensors. The dot was a drop of precursor solution after UV exposure and drying. The expanded picture on the right shows the detail of a bare array element.

The response of the PANI-nanometal composite sensors to triethylamine vapor in nitrogen gas showed that bulk PANI was the least sensitive and slowest to respond. Improvements in sensitivity and response rates were found with PANI nanofibers. Additional improvement was found with the incorporation of nanometal particles, with Ag particles being the most sensitive. The response to the triethylamine was fit to an exponential function or:

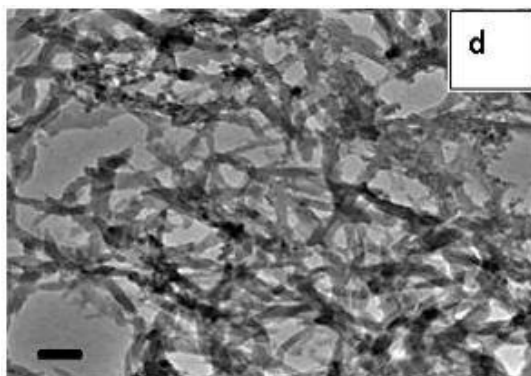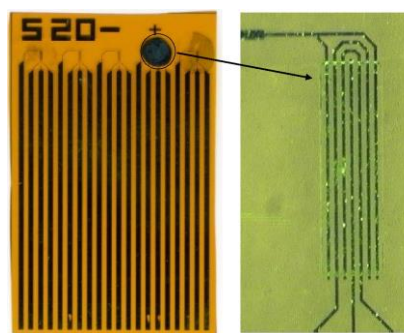$$I_{norm}(t) = (1 - I_\infty) \exp(-t/\tau) + I_\infty \qquad (1)$$

Fig. 2. PANI nanofibers (mesh) after irradiation of the precursor solution [5]. The scale bar in "d" is for 100 nm.

where the I's represent the currents at various times, t, and is the time constant for the signal reduction. PANI nanofiber-Ag sensors were 20 times more sensitive and 4 times faster than bulk PANI sensors. The reason for the enhanced sensitivity was revealed by Raman spectroscopy, which showed that there was a charge transfer from the PANI to the Ag particle when dopant (acid) was present. This charge transfer was diminished in the presence of the triethylamine. It therefore appears, that the Ag particles act similar to a dopant, giving rise to the enhanced response.

The behavior of these sensors was modeled based on a surface adsorption and Langmuir adsorption model [6]. For surface adsorption, a

dual sorption model and adequately fit the data. Each model gave different and useful insight into the physics of the systems [6]. The dual sorption model suggested the presence of diffusive and non-diffusive holes. The diffusion model, was consistent with the notion that the diffusion of the de-dopant to the dopant controlled the response rate.

Because of their low cost, environmentally friendly synthesis, and ease of preparation, we believe that these materials have significant potential for a variety of applications. However, there are still a number of things that need to be understood before these materials can reach this potential.

The behavior of adsorbed surfactant cetyltrimethylammonium bromide (CTAB) on silica was studied by temperature-modulated d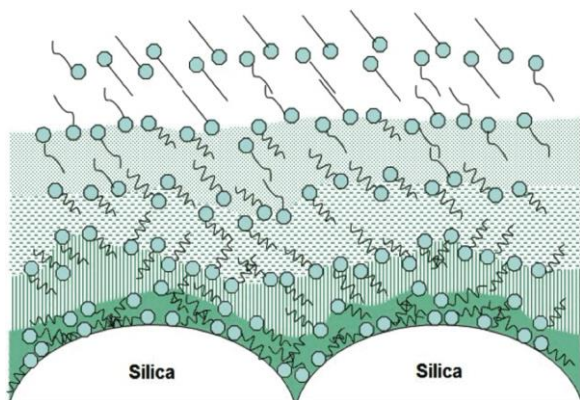ifferential scanning calorimetry (TMSDC), thermogravimetric analysis (TGA), Fourier transform infrared spectroscopy (FTIR) and powder X-ray diffraction. The results were interpreted with a layered model [7]. CTAB association structures were found for the adsorption of surfactant on the silica surface namely: a monolayer, a second layer that completed a bilayer, and multilayer structures. The silica surface was found to lower both the melting and crystallization temperatures of the CTAB tails. The enthalpy and entropy changes for CTAB during the melting and crystallization indicate that the CTAB molecules underwent significant structural changes, from surface to bulk-like structures. The first layer of CTAB on silica was rather disordered, followed by a more ordered bilayer, followed by layers that approach bulk-like (well ordered) behavior. This understanding helped us understand the behavior of polymers made in the room temperature polymerization of emulsion gels. A schematic structure of the CTAB near the surface is shown in Figure 3.

Fig. 3. Schematic structure of adsorbed CTAB on silica showing an increased organization as the distance from the surface increases. The layout for the CTAB molecules was based on consideration of a monoclinic lattice of CTAB crystals.

References

[1] Werake; L. K.; Story; J. G.; Bertino; M. F.; Pillalamarri; S. K.; Blum, F. D. "Photolithographic synthesis of polyaniline nanofibres," *Nanotechnology* **2005**, *16*, 2833-2837.

[2] Pillalamarri; S. K.; Blum; F. D.; Tokuhiro; A. T.; Story; J. G.; Bertino, M. F. "Radiolytic synthesis of polyaniline nanofibers: A new templateless pathway," *Chem. Mater*. **2005**, *17*, 227-229.

[3] Pillalamarri, S. K.; Blum, F. D.; Tokuhiro, A. T.; Bertino, M. F. "One-pot Synthesis of Polyaniline-Metal Nanocomposites," *Chem. Mater.* **2005**, *17*, 5941-5944.

[4] Li; Z. F.; Blum; F. D.; Bertino; M. F.; Kim; C. S.; Pillalamarri, S. K. "One-step fabrication of a polyaniline nanofiber vapor sensor," *Sens. Actuators, B* **2008**, *134*, 31-35.

[5] Li, Z. F.; Blum, F. D.; Bertino, M. F.; Kim, C. S. "Amplified response and enhanced selectivity of metal-PANI fiber composite based vapor sensors," *Sens. Actuators, B* **2012**, *161*, 390-395.

[6] Li, Z.-F.; Blum, F. D.; Bertino, M. F.; Kim, C.-S. "Understanding The Response of Nanostructured Polyaniline Gas Sensors," *Sens. Actuators, B* **2013**, *183*, 419-427.

[7]   Zhang, T.; Xu, G.; Puckette, J.; Blum, F. D. "Effect of Silica on the Structure of Cetyltrimethylammonium Bromide," *J. Phys. Chem. C* **2012**, *116*, 11626−11634.

Regioselective Cross-Linking of Silica Aerogels with Magnesium Silicate Ceramics

Professor Massimo Bertino

Department of Physics, Virginia Commonwealth University (VCU)

The VCU team developed a fabrication method, which allows one to mechanically reinforce aerogels without compromising their porosity since the core retains the characteristics of native aerogels [1]. The reinforcement is ceramic in nature (mainly magnesium silicate) and it is stable at temperatures comparable to the densification temperature of silica aerogels (~900 $^{\circ}$C), which are much higher than the temperatures (~200 $^{\circ}$C) accessible to polymer-reinforced aerogels. Cross-linking depends on the presence of carbon in the aerogel structure. We obtained cross-linking only when carbonization conditions had been fulfilled, that is, PAN was used as a crosslinker, oxidized at 225 $^{\circ}$C in air and then heated to the carbonization temperature of 850 $^{\circ}$C. Masking allows one to reinforce only selected parts of aerogels and it could be employed to integrate aerogels into mechanical assemblies by reinforcing only the regions most subject to mechanical stress. Our results may also allow development of non-aerogel ceramic materials with anisotropic physical and chemical composition. In our process, chemical and physical properties are altered within the same monolith by introducing a catalyst (carbon in our case) for a solid-state reaction using conventional lithographic methods. The flexibility of lithography allows in principle to generate complicated patterns, which are not accessible to conventional methods of fabrication of anisotropic ceramics such as layering, bonding and generation of temperature and/or chemical gradients during processing.
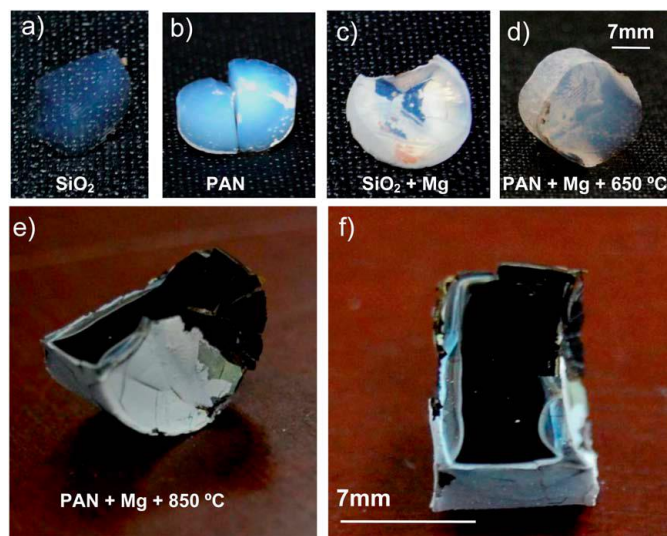

Fig. 1. Digital camera images of: (a) a native silica aerogel processed at 850 $^{\circ}$C without Mg, (b) a X-PAN aerogel processed at 850 $^{\circ}$C without Mg, (c) a Mg-native aerogel, (d) a Mg-PAN aerogel processed at 650 $^{\circ}$C; (e and f) a Mg-PAN aerogel processed at 850 $^{\circ}$C.

References

[1] Franzel, L.; Wingfield, C.; Bertino, M.F.; Mahadik-Khanolkar, S.; Leventis, N. "Regioselective cross-linking of silica aerogels with magnesium silicate ceramics," *J. Mater. Chem. A* **2013**, *1*, 6021-6029.